

1 **Xylem and phloem in petioles are coordinated with leaf gas exchange in oaks with**
2 **contrasting anatomical strategies depending on leaf habit**

3 Rubén Martín-Sánchez*¹, Domingo Sancho-Knapik^{1,2}, Juan Pedro Ferrio³, David Alonso-Forn⁴, Juan
4 Manuel Losada⁵, José Javier Peguero-Pina^{1,2}, Maurizio Mencuccini^{6,7}, Eustaquio Gil-Pelegrín³

6 ¹Departamento de Sistemas Agrícolas, Forestales y Medio Ambiente, Centro de Investigación y
7 Tecnología Agroalimentaria de Aragón (CITA), Avda. Montañana 930, 50059, Zaragoza, Spain

8 ²Instituto Agroalimentario de Aragón -IA2- (CITA-Universidad de Zaragoza), Zaragoza, Spain

9 ³Estación Experimental de Aula Dei, Consejo Superior de Investigaciones Científicas (EEAD-CSIC),
10 Avda. Montañana 1005, Zaragoza 50059, Spain

11 ⁴Research Group on Plant Biology Under Mediterranean Conditions, Department of Biology, University
12 of Balearic Islands (UIB). Ctra Valldemossa km 7,5 E-07122 Palma, Balearic Islands, Spain.

13 ⁵Institute for Mediterranean and Subtropical Horticulture -La Mayora- (IHSM La Mayora—CSIC—
14 UMA), Avda. Dr. Wienberg s/n, 29750 Malaga, Spain

15 ⁶CREAF, Campus UAB, Cerdanyola del Vallés, Spain

16 ⁷ICREA, Barcelona, Spain

18 * Corresponding author: Rubén Martín-Sánchez

20 **Email addresses** of all the authors

21 RMS: rmartin@cita-aragon.es

22 DSK: dsancho@cita-aragon.es

23 JPF: jpferrio@eead.csic.es

24 DAF: david.alonso@uib.es

25 JML: juan.losada@csic.es

26 JJPP: jjpeguero@cita-aragon.es

27 MM: m.mencuccini@creaf.uab.cat

28 EGP: gilpelegrin@eead.csic.es

30 **ORCID identifier** of authors (for non-ambiguous identification of authors)

32 Rubén Martín-Sánchez: 0000-0002-0288-3869

33 Domingo Sancho-Knapik: 0000-0001-9584-7471

34 Juan Pedro Ferrio: 0000-0001-5904-7821

35 David Alonso-Forn: 0000-0002-1467-1943

36 Juan Manuel Losada: 0000-0002-7966-5018

37 Jose Javier Peguero-Pina: 0000-0002-8903-2935

38 Maurizio Mencuccini: 0000-0003-0840-1477

39 Eustaquio Gil-Pelegrín: 0000-0002-4053-6681

41 **Keywords:** Conductive tissues, hydraulic conductivity, petioles, *Quercus*, leaf habit,
42 stomatal conductance, photosynthesis

44 ABSTRACT

45 As the single link between leaves and the rest of the plant, petioles must develop
46 conductive tissues according to the water influx and sugar outflow of the leaf lamina. A
47 scaling relationship between leaf area and anatomical traits of xylem and phloem is
48 expected to improve the efficiency of these tissues. However, the different constraints
49 compromising the functionality of both tissues (e.g., risk of cavitation) must not be
50 disregarded. Additionally, plants present two main leaf habits (deciduous and evergreen)
51 that may have different strategies to produce and package their petiole conduits to cope
52 with environmental restrictions. In this study, we explore, in a diverse group of 33 oak
53 species, the relationships between petiole anatomical traits, leaf area, stomatal
54 conductance and photosynthesis rate. Results showed allometric scaling between
55 anatomical structure of xylem and phloem with leaf area. We also found how
56 photosynthesis and stomatal conductance at leaf-level are correlated with anatomical
57 traits in the petiole. Nonetheless, the main novelty is how oaks present a different strategy
58 depending on the leaf habit. Deciduous species tend to increase their diameters to achieve
59 a greater leaf-specific conductivity. By contrast, evergreen oaks develop larger xylem
60 conductive areas for a given leaf area than deciduous ones. This trade-off between safety-
61 efficiency in petioles has never been attributed to the leaf habit of the species.

62

63 INTRODUCTION

64 Petioles, besides accomplishing a structural function, link the main photosynthetic organs
65 —i.e., leaf laminae— with the rest of the plant. In this regard, they may act as a bottleneck
66 in the soil-plant-atmosphere continuum for water transport and the translocation of
67 photosynthates (Brocious and Hacke, 2016). Thus, transpiration has been traditionally
68 related to transport capacity of xylem and photosynthesis rate to export capacity of
69 phloem in petioles (Salisbury, 1913; Brocious and Hacke, 2016). However, this
70 correlation has been questioned within angiosperms (Gleason et al., 2016). These authors
71 reported a weak or even absent coordination between hydraulic capacity and gas
72 exchange capacity.

73 Petioles must contain enough xylem vessels and sieve tubes to, respectively, supply water
74 to the leaf lamina and export assimilates from the leaf to the rest of the plant. For this
75 reason, a scaling relationship between leaf area and both xylem and phloem structures
76 (area of conductive tissues and size of the conduits) in petioles is expected (Ray and
77 Jones, 2018). The number and size of the conduits ultimately reflects the transport ability
78 —namely, the hydraulic conductivity (K_h)— of the conductive tissues according to the
79 Hagen-Poiseuille law (Tyree and Zimmermann, 2002; Hirose et al., 2005; Woodruff,
80 2014). Nonetheless, the K_h only shows how much fluid is potentially able to be moved
81 along a pathway whereas two petioles with the same K_h can support different leaf areas.
82 For this reason, the leaf-specific conductivity (LSC) of a petiole provides a more
83 physiological explanation of a leaf's efficiency as LSC is the capacity to supply water (K_h)
84 per leaf area. LSC can also be expressed as the product of the specific conductivity (K_s ,
85 i.e. K_h per conductive area ratio) and the Huber value (H_v , i.e. conductive area per leaf
86 area ratio) (Mencuccini et al., 2019). Therefore, the same LSC can be achieved in different
87 ways by modulating both K_s and H_v . Indeed, Mencuccini et al. (2019) found in a wide
88 range of plant species a negative relationship between K_s and H_v in stems. What are the
89 implications of increasing each variable?

90 Increasing the Huber value, that is, allocating more cross-sectional area to a conductive
91 function, would imply a reduction in the availability of space for structural support. This
92 could result in a possible trade-off between both kind of tissues (Zwieniecki et al., 2004).
93 By contrast, as the specific conductivity mainly depends on the diameter of the conduits,
94 the hydraulic capacity of the petiole is compromised by the same factors that determine
95 its vulnerability, as in any other parts of the plant (Hacke and Sauter, 1996) In fact, it has

96 been suggested that petioles may act as hydraulic fuses for the plant through higher
97 vulnerability to embolism than stems, thereby ensuring resilience to extreme drought
98 events (Peguero-Pina et al., 2015; Alonso-Forn et al., 2021). Throughout their lifespan,
99 leaves can be affected by climatic stresses (e.g. aridity or cold) that may influence the size
100 of the xylem conduits (Gil-Pelegrín et al., 2017). In this sense, many studies showed a
101 higher vulnerability to cavitation in species with wider vessels (Hacke et al., 2000; Tyree,
102 2003; Hacke et al., 2006; Cai and Tyree, 2010; Jacobsen et al., 2019; Blackman et al.,
103 2023). Embolized xylem conduits leads to hydraulic failure, which is the main cause of
104 plant mortality in response to drought (Tyree and Sperry, 1989). By contrast, many species
105 inhabiting very stressful habitats reduce the diameter of their conduits, achieving a higher
106 resistance to cavitation. This reduction in the conduit diameter results in a lower water
107 transport efficiency (Giordano et al., 1978). However, this decrease may be compensated
108 by increasing the number of conduits (Nardini et al., 2012). When cavitation is caused by
109 freeze-thaw cycles, the same arguments arise. Wider conduits are likewise more
110 vulnerable than small ones because they contain greater dissolved air which can form
111 larger bubbles causing cavitation at lower tensions (Cochard and Tyree, 1990; Sperry and
112 Sullivan, 1992; Lo Gullo and Salleo, 1993; Lemoine et al., 1999; Sevanto, et al., 2012;
113 Zanne et al., 2014; Ni et al., 2022).

114 Regarding the phloem, other factors rather than climatic stresses might influence the size
115 of its conduits. Sugars, amino acids and other organic metabolites in the sap make sieve
116 tubes a target for some phytophagous insects like aphids (Will et al., 2013). When an
117 aphid stings a sieve tube with its stylet, the plant responds by occluding the sieve plates
118 with callose, turning it into a non-functional conduit (Will and van Bel, 2006). Thus,
119 building more but smaller sieve elements is safer than building a few large conduits
120 (Ewers and Fisher, 1991). Besides, wider sieve elements would need to load more sugars
121 in the source (i.e., the leaf), to generate enough turgor pressure gradient for sap to flow
122 towards the sink organs (Hölttä et al., 2009; Sevanto, 2014).

123 The scaling relationship between xylem and phloem areas has been explored in several
124 species (Jyske and Hölttä, 2015; Carvalho et al., 2017a; Carvalho et al., 2017b;
125 Kiorapostolou and Petit, 2018; Ray and Jones, 2018; Losada et al., 2022). Most of the
126 studies focus on stems, although Ray and Jones (2018) analyzed petioles in several
127 *Pelargonium* species. Albeit plants tend to present more xylem than phloem, an
128 isometrical scaling has been found in these studies. Nonetheless, most research focuses

129 on a single species. To our knowledge, they do not conduct comparative analyses across
130 different leaf longevities, even in genus level studies. Deciduousness and evergreenness
131 offer different solutions to cope with climatic stresses, which are, in turn, closely related
132 to specific leaf area (SLA) (Sancho-Knapik et al., 2021) (Fig. 1). Similarly, these climatic
133 stresses have been demonstrated to limit the growth of the conduits, even in petioles
134 (Blackman et al., 2023). Since the LSC ultimately depends on the leaf area, the Huber
135 value and the diameter of the conduits, we wonder if the two different leaf habits could
136 develop two different strategies (Fig. 1, models A and B) to reach similar values of LSC.

137 The genus *Quercus* (oaks) offers an excellent system to study the scaling between both
138 conductive tissues, xylem and phloem, besides its ecophysiological implications. Oaks
139 represent a single monophyletic clade with over 400 species occupying very different
140 habitats around the northern hemisphere, from tropical rainforests to cold temperate
141 forests through semideserts and chaparrals. Additionally, oak species exhibit a much
142 broader range not only in terms of leaf area, but also in leaf lifespan compared to other
143 widely studied genera such as *Populus*, *Pelargonium* or *Eucalyptus* (Brocius and Hacke,
144 2016; Ray and Jones, 2018; Blackman et al., 2023). The variability in leaf area can
145 suppose a difference of 70 times between the species with the largest and the smallest
146 leaves (Sancho-Knapik et al., 2021). Finally, phenology ranges from deciduous with a
147 lifespan of just five months up to evergreen species whose leaves can persist over several
148 years (Mediavilla et al., 2008; Harayama et al., 2016).

149 In this study we explore the scaling relationships among the different xylem and phloem
150 traits in petiole cross-sections, leaf area, stomatal conductance, photosynthesis rate and
151 climatic variables in 33 oak species (16 deciduous and 17 evergreen) covering the full
152 range of variation in oaks in terms of leaf area and leaf habit. Based on the information
153 presented thus far (Fig. 1), four aims were addressed: 1) to explore the scaling
154 relationships between conductive tissue structures in petioles —i.e., conductive area and
155 hydraulic diameter of the conduits— and leaf area, for both xylem and phloem; 2) to
156 verify whether deciduous and evergreen species exhibit the same LSC, and to check if
157 deciduous and evergreen oaks follow a different strategy when producing and packaging
158 their conduits to improve their efficiency; 3) in case that two different models are
159 observed, to relate them with climatic variables (mainly aridity and cold) that could be
160 explaining such differences; 4) to assess if the hydraulic architecture resulting from the
161 observed scaling correlates with the physiological demands of the leaf, i.e., stomatal

162 conductance and photosynthesis rate. We hypothesized that xylem and phloem petiole
163 traits should scale proportionally with leaf area, which ultimately reflects the water
164 demands (stomatal conductance) and export requirements (photosynthesis rate) of the leaf
165 lamina.

166

167 MATERIAL AND METHODS

168 *Plant material*

169 In this study, we sampled 22 oak species occurring in the living collection in CITA de
170 Aragón (41°39'N, 0°52'W, 200 m a.s.l., Zaragoza, Spain). In order to get a greater
171 diversity of species and to cover a wider range of leaf areas, we also sampled 11 additional
172 species from Jardín Botánico de Iturrarán 43°15'N 2°09.3'W, 200 m a.s.l., Gipuzkoa,
173 Spain).

174 We sampled five mature leaves of south-exposed branches from 3-5 trees per species.
175 They were sealed in plastic bags and carried to the laboratory. The mid-section of the
176 petiole was cut and stored in 70% ethanol. Then, leaf area (LA) was measured using
177 ImageJ software by scanning the leaf lamina.

178

179 *Anatomical traits*

180 Petiole sections were dehydrated in a graded ethanol series and subsequently embedded
181 in Paraplast Plus embedding medium (Leica, Richmond, IL, USA). The resulting paraffin
182 blocks were cut in the microtome (HM 350S; MICROM, Walldorf, Germany) to obtain
183 15-20 μm cross-sections that were stained with saffranine (0.1% w/v), picric acid (0.5%
184 v/v) and AstraBlue (0.1% w/v) after being deparaffinated with Isoparaffin H and
185 rehydrated using a graded ethanol series (100, 95, 90 and 70 %). Then, sections were
186 observed and photographed under a light microscope (OPTIKA B-600TiFL; Optika
187 Microscopes, Ponteranica, Italy) (Fig. 2). We measured the total petiole cross-sectional
188 area (A_{pet}), as well as the conductive area, i.e., the sum of xylem and phloem areas (Fig.
189 2a). Hereafter, we will use conductive area (A_c) to refer to the sum of the two vascular
190 tissues and we will distinguish between xylem area (A_x) and phloem area (A_p) when
191 treated separately. Besides, we measured the total number of xylem vessel elements and
192 phloem conduits and their mean diameter in three subsamples of the whole conductive

193 area of each tissue per photograph (Fig. 2b, 2c). In the phloem, our aim was to measure
 194 only sieve tubes; however, we cannot claim to have exclusively measured these ones since
 195 a visible sieve tube plate (or their identification with callose staining) is necessary to
 196 properly identify a sieve tube. We discarded the first brick-shaped cell layers (i.e., the
 197 procambium). Medullary rays and cells with a visible nucleus and organelles were also
 198 neglected. Finally, very small cells (what we interpret as companion cells or oblique/bevel
 199 cuts) as well as the big rounded thick-wall cells in the distal part of the phloem (phloem
 200 fibers) were also avoided (Esau, 1939). The rest of the cells were considered as potentially
 201 sieve tubes and as such, measured. Afterwards, we calculated the hydraulic diameter for
 202 xylem (d_{hx}) and phloem (d_{hp}) using the formula proposed by Sperry et al. (1994):

$$203 \quad d_h = \frac{\sum_i d_i^5}{\sum_i d_i^4}$$

204 where d_i is the mean diameter of each conduit measured. Then, we also calculated the
 205 ratio of the conductive area normalized by the leaf area following the next formula:

$$206 \quad \text{For xylem: } XLA = \frac{A_x}{LA \times 10000} \quad ; \quad \text{For phloem: } PLA = \frac{A_p}{LA \times 10000}$$

207

208 Where A_x is the total xylem area, A_p is the total phloem area and LA is leaf area. Leaf area
 209 was multiplied by 10 000 to obtain values close to one and to transform units to $\text{cm}^2 \text{m}^{-2}$.
 210 All measurements were done using ImageJ software. Traits analyzed are compiled in
 211 Table 1.

212

213 *Hydraulic conductivity*

214 We calculated the theoretical hydraulic conductivity of the whole petiole (K_h) as the sum
 215 of each conduit conductivity assuming that both types, xylem vessels (K_{hx}) and phloem
 216 cells (K_{hp}), follow the Hagen-Poiseuille law (Tyree and Zimmermann, 2002; Hirose et al.,
 217 2005; Woodruff, 2014):

$$218 \quad K_h = \sum_i \frac{d_i^4 \pi \rho}{128 \eta}$$

219 where ρ is the density of the fluid moving along the conduits at 25 °C, assuming pure
220 water for xylem (997kg m⁻³) and a specific sap density dependent of sucrose concentration
221 for phloem (1068 kg m⁻³) (Jensen et al., 2013), η is the viscosity of the fluid at 25 °C, pure
222 water for xylem (8.9 x 10⁻¹⁰ MPa s) and 1.91 times that value for phloem sap (1.7 x 10⁻⁹
223 MPa s) (Thomson, 2006; Jensen et al., 2013); and d_i is the mean lumen diameter of each
224 conduit.

225 Additionally, we calculated leaf-specific hydraulic conductivity of xylem (LSC):

$$226 \quad LSC = \frac{K_{hx}}{LA}$$

227 where LA is leaf area. We also calculated the specific conductivity for xylem (K_{sx}):

$$228 \quad K_{sx} = \frac{K_{hx}}{A_x}$$

229 where A_x is the area of xylem in the cross-section of the petiole.

230

231 *Climatic variables*

232 To get a mean representative value of different climatic variables for each species we
233 followed the same procedure as in Martín-Sánchez et al. (2024). In short, we first
234 downloaded GBIF individual presence points for the 33 species studied, we thinned the
235 data to one presence point per square kilometer using SDMtune R package (Vignali et al.,
236 2020) and we extracted the climatic variables from the WorldClim version 2.1 database
237 (Fick and Hijmans, 2017. WorldClim 2. <https://www.worldclim.org>). We additionally
238 added an aridity index (AI) calculated as mean annual precipitation (MAP) divided by
239 potential evapotranspiration (PET) (Mencuccini et al., 2019; Peguero-Pina et al., 2020).
240 All individual values were summarized into a mean value for each species. To test our
241 hypothesis whether hydraulic diameters are restrained by climatic factors, we chose
242 variables related to cold and aridity: mean annual temperature (MAT), mean of daily
243 minimum temperatures during the coldest quarter (T_{min}), mean annual precipitation
244 (MAP) and the aridity index (AI).

245

246 *Leaf gas exchange*

247 We obtained the mean photosynthesis rate (A_N) and stomatal conductance (g_s) of 26
248 species. For nine species, we measured these parameters using an open gas exchange
249 system (CIRAS-3, PP-Systems, Amesbury, MA, USA) fitted with an automatic universal
250 leaf cuvette (PLC6-U, PP-Systems, Amesbury, MA, USA) in six leaves per species from
251 our living collection. All measurements were conducted under the following standard
252 environmental conditions: CO₂ concentration surrounding the leaf (C_a) of 400 $\mu\text{mol mol}^{-1}$,
253 leaf temperature of 25 °C, vapor pressure deficit of 1.25 kPa and saturating
254 photosynthetic photon flux density of 1500 $\mu\text{mol m}^{-2} \text{s}^{-1}$. We complemented our own
255 measurements with data for 17 species compiled from other studies (Vaitkus and McLeod,
256 1995; Nagel et al., 2002; Thadani et al., 2009; Huang et al., 2016; Llusia et al., 2016;
257 Jafarnia et al., 2018; Alonso-Forn et al., 2020; Kar et al., 2021). Assuming a mean value
258 of A_N and g_s for each species and taking into account the mean LA measured for each
259 species, we calculated the theoretical mean photosynthesis rate and stomatal conductance
260 at whole leaf level. ($A_{N,leaf}$ and $g_{s,leaf}$, respectively).

261

262 *Statistical analyses*

263 First, we tested the potential effect of the garden throughout several analyses of variance
264 (ANOVAs) and linear regressions via mixed models. On the one hand, we performed
265 ANOVAs for each single trait to see how much variance was explained by species and
266 the garden (Table S1). On the other hand, we did linear regressions via mixed models
267 including the garden as a random factor in correlations between pairwise traits, besides a
268 subsequent ANOVA to see how much variance is explained by the random factor.
269 Variance explained by garden in the first ANOVA showed that, for every trait, species
270 accounted for more variance than the garden and in most of the cases species accounted
271 over 60% of variance. Besides, correlations remain significant even when garden is
272 included as a random factor (Table S2). Finally, when we tested differences in the leaf
273 habit, we additionally accounted for garden and the interaction between leaf habit and
274 garden in the ANOVAs. In most of the cases, the interaction resulted to be non-significant,
275 except for three traits (Table S3). Even among those exceptions leaf habit and/or residuals
276 accounted for more variance than the garden. In view of these results, we conclude that
277 correlations are not strongly skewed by an effect of the garden.

278 Cross-correlations were performed between the different anatomical, hydraulic and
279 physiological traits, assuming a log-log correlation. Alternatively, linear cross-
280 correlations were performed between xylem and phloem hydraulic diameters and climatic
281 variables. Post-hoc analyses of every regression fit were performed using DHARMA R
282 package to test normality, homoscedasticity and outliers (Hartig, 2022). Additionally, we
283 used SMATR R package to check if the scaling relationships were isometric or allometric
284 (Warton et al., 2012). This calculates the slope for the bivariate linear relationship
285 between two variables (after being \log_{10} -transformed) following the standardized major
286 axis regression. If the 95% confidence interval of the slope includes the value of 1,
287 isometry cannot be rejected, whereas allometry can be assumed when this confidence
288 interval does not include such value. For anatomical traits and conductivities, we
289 performed slope tests including leaf habit as factor. Finally, for physiological traits, all
290 species were considered together.

291

292 RESULTS

293 The range of variation covered in this study in terms of leaf area goes from 1.9 cm²
294 (*Quercus monimotricha*) up to 151 cm² (*Quercus macrocarpa*). If species are compared
295 by their leaf habit, significant differences ($P < 0.001$) can be found between deciduous
296 (DEC; 68.7 ± 46 cm²) and evergreen (EVE; 16.6 ± 15 cm²) (Fig. 3a). Raw measurements
297 of all the measured diameters are represented as a violin plot to notice the range of
298 variation either between leaf habits or between conductive tissues (Fig. 3b). Hydraulic
299 diameter (d_h) is always significantly wider — either for xylem (d_{hx}) or phloem (d_{hp}) — in
300 deciduous than in evergreen species although the range of variation in xylem vessels
301 diameter (25 ± 7.64 μ m in deciduous; 15.8 ± 5.6 μ m in evergreen) is higher than in phloem
302 cells diameter (8.19 ± 1.77 μ m in deciduous; 6.28 ± 1.42 μ m in evergreen). When the
303 conductive area (A_c) is examined (Fig. 3c), deciduous species also display larger xylem
304 and phloem cross-sectional areas ($A_x = 297 \pm 180 \times 10^3$ μ m², $A_p = 224 \pm 147 \times 10^3$ μ m²)
305 compared to evergreen species ($A_x = 175 \pm 121 \times 10^3$ μ m², $A_p = 128 \pm 116 \times 10^3$ μ m²)
306 (Fig. 2c). Nonetheless, the ratio between cross-sectional areas of the vascular elements in
307 the petiole and LA —i.e., XLA and PLA —, reveals significantly lower values in
308 deciduous species (XLA = 4628 ± 1371 , PLA = 3885 ± 2320) compared with evergreen
309 species (XLA = 14207 ± 9038 , PLA = 9242 ± 3923) (Fig. 3d), which means that evergreen
310 oaks have a higher conductive area per leaf area. Calculated xylem hydraulic conductivity

311 (K_{hx}) and xylem specific conductivity (K_{sx}) also present highly significant ($P < 0.001$)
312 differences between deciduous and evergreen species. By contrast, K_{hp} does not show
313 significant differences when leaf habit is considered ($P = 0.902$) (Table 2).

314 Although the cross-sectional petiole (A_{pet}) area shows a positively significant relationship
315 with LA ($P < 0.001$), the dispersion of the data is quite high, especially in deciduous
316 species (DEC: $R^2 = 0.486$, EVE $R^2 = 0.752$) (Fig. 4a). Conductive area (A_c) presents a
317 strong correlation with LA for both leaf habits ($P < 0.001$, DEC: $R^2 = 0.816$, EVE $R^2 =$
318 0.816) (Fig. 4b, Table 3).

319

320 *Xylem and phloem anatomy*

321 We analyze how the conductive area of both tissues, xylem and phloem, as well as the
322 hydraulic diameter of conduits scale with leaf area. In all cases, traits scale positively and
323 significantly ($P < 0.001$) with LA (Fig. 5, Table 3). The larger a leaf is, the larger is the
324 investment in conductive area (Fig. 5a, d) and wider conduits (Fig. 5b, e). However, the
325 relationships are not linear but logarithmic, so that for small leaves, a slight increment in
326 leaf area implies a big increase in both, A_c and d_h , especially in evergreen species. Xylem
327 and phloem also present the same behavior when their ratios are analyzed, i.e., how much
328 A_x and A_p a petiole develops divided by leaf area (Fig. 5c, f). XLA and PLA scale
329 negatively and significantly ($P < 0.001$) with LA either for deciduous or evergreen species
330 (Fig. 5c, f). Evergreen species show a huge heterogeneity in their ratio values for both
331 xylem and phloem for the smallest values of LA. In other words, there is a group of small-
332 leaved evergreen species that invests more in A_x for a specific LA in comparison to large-
333 leaved evergreen leaves. XLA and PLA values above a LA of c.a. 50 cm^2 become
334 asymptotical. The scaling relationships are allometric in all cases (Table 3).

335 When both conductive areas are correlated, a strong linear relationship ($P < 0.001$) can be
336 appreciated (Fig. S1; $R^2 = 0.716$ for DEC, $R^2 = 0.811$ for EVE). When leaf habit is taken
337 into account, the scaling for deciduous species can be considered isometric (Fig. S1). By
338 contrast, evergreen species present an allometric scaling between A_x and A_p , with more
339 xylem produced than phloem (Fig. S1).

340

341 *Petiole hydraulic conductivity*

342 Calculated hydraulic conductivity of xylem (K_{hx}), i.e., the theoretical capacity of the
343 whole petiole to supply water to the leaf, results to be positively and significantly ($P <$
344 0.001 , DEC: $R^2 = 0.724$, EVE $R^2 = 0.560$) correlated with LA (Fig. 6a). Deciduous species
345 with the largest leaves present up to ten-fold higher values of K_{hx} than the evergreen ones
346 with the lowest values (Fig. S2a). For both leaf habits an allometric relationship between
347 K_{hx} and LA is supported (Table 3).

348 The specific conductivity of xylem (K_{sx}) also presents a high significance ($P < 0.001$) in
349 both groups in relation with LA, although correlations are much weaker in comparison to
350 K_{hx} , especially for evergreen species (DEC: $R^2 = 0.415$, EVE: $R^2 = 0.281$) (Fig. 6b, Table
351 3). Deciduous species present significant higher values of K_{sx} than evergreen ones (Fig.
352 S2b). In this case, isometry cannot be rejected for either deciduous or evergreen species
353 (Table 3). Leaf-specific conductivity (LSC) is significantly higher in deciduous species
354 than evergreen ones ($P < 0.001$) (Fig. S2c).

355 Calculated phloem hydraulic conductivity (K_{hp}) is in all cases much lower than for xylem
356 with weaker or non-significant correlations with LA (DEC: $R^2 = 0.276$, $P = 0.06$; EVE:
357 $R^2 = 0.036$, $P = 0.55$) (Table 3, plot not shown). It is over 100 times lower than the K_{hx} on
358 average for deciduous species (data not shown). Differences among evergreen species are
359 less remarkable, with a K_{hx} c.a. 20 times higher than K_{hp} on average and some specific
360 individuals with a similar conductivity for both conductive tissues (data not shown).

361 When XLA is compared with the K_{sx} (Fig. 7a), it can be noticed how deciduous species,
362 whose leaves are larger, hardly present variation in their XLA values. By contrast they
363 display a wide range of values in their K_s . Conversely, evergreen species show a wide
364 range of variation in their XLA values without an apparent increase in their K_{sx} , with the
365 exception of *Q. costaricensis*, which is, in turn, among the species with the largest leaves
366 within evergreen oaks.

367 Similarly, in the comparison between XLA with the respective d_{hx} (Fig. 7b), it can be seen
368 how individuals tend to contribute mainly to one axis depending on their leaf habit. This
369 is, deciduous species basically present much higher range of variation in d_{hx} than in XLA.
370 By contrast, evergreen oaks present a larger variation in XLA than in d_{hx} . Both increments,
371 either in d_{hx} or in XLA leads to an improvement in the LSC, although species that increase
372 their d_{hx} , represented by deciduous oaks, improve their LSC more than evergreen oaks
373 that increase their xylem area.

374

375 *Climatic correlations*

376 Mean annual precipitation reveals a significant relationship with d_{hx} for evergreen species
377 ($P = 0.02$) but no significance is found in deciduous ($P = 0.07$). Taking into account the
378 potential evapotranspiration, i.e., comparing the aridity index (AI) with d_{hx} improves the
379 relationships. Aridity index shows positive correlation with d_{hx} for both deciduous ($P =$
380 0.03 ; $R^2 = 0.249$) and evergreen species ($P = 0.02$; $R^2 = 0.274$) (Fig. S3). The smallest
381 hydraulic diameters are displayed in the most xeric species. Regarding temperature, MAT
382 does not seem to be significantly related to d_{hx} either for deciduous ($P = 0.24$) or evergreen
383 species ($P = 0.91$). Conversely, T_{min} was only compared for evergreen species since
384 deciduous oaks lack leaves during winter. The correlation did not present significance (P
385 $= 0.37$; Fig. S4).

386

387 *Relationships between vascular traits, stomatal conductance and photosynthesis net rate*

388 When the main attributes of the xylem in the petiole are correlated with the stomatal
389 conductance at leaf level ($g_{s,leaf}$), significant relationships can be appreciated in all cases
390 ($P < 0.001$) (Fig. 8). There is a significant increase in $g_{s,leaf}$ as A_x becomes larger with an
391 allometric relationship ($R^2 = 0.512$) (Fig. 8a, Table 4). For a given value of A_x , deciduous
392 species tend to present higher values of $g_{s,leaf}$ than evergreen ones. Stomatal conductance
393 also increases allometrically as d_{hx} becomes wider, but with a steeper slope ($R^2 = 0.586$)
394 (Fig. 8b, Table 4). Likewise, deciduous species usually present higher values of $g_{s,leaf}$ for
395 the same d_{hx} than evergreen ones. Once again, K_{hx} also scaled allometrically (Fig. 8c,
396 Table 4) and deciduous species have higher values than evergreen species on average.

397 When the same xylem traits are correlated with the photosynthesis net rate, exactly the
398 same trends arise (Table 4). The $A_{N,leaf}$ appears to be related to A_x (Fig. 8d, $P = 0.001$, R^2
399 $= 0.591$), d_{hx} (Fig. 8e, $P < 0.001$, $R^2 = 0.671$) and K_{hx} (Fig. 8f, $P < 0.001$, $R^2 = 0.786$).

400 Photosynthesis net rate at leaf level ($A_{N,leaf}$) is significantly correlated with phloem
401 anatomical traits ($P < 0.001$) (Fig. 9, Table 4). $A_{N,leaf}$ increases with larger A_p ($R^2 = 0.561$)
402 (Fig. 9a) and wider d_{hp} ($R^2 = 0.509$) (Fig. 9b) being on both cases an allometric
403 relationship. Deciduous species tend to present higher photosynthesis net rates at leaf

404 level than evergreen ones. Finally, the relationship between $A_{N,leaf}$ and K_{hp} is barely
405 significant ($P = 0.043$) with a very weak correlation ($R^2 = 0.130$) (plot not shown).

406

407 DISCUSSION

408 *Anatomical traits scale with leaf area*

409 In the *Quercus* species studied, we found associations between the anatomical traits of
410 the petioles and leaf area. First, the cross-sectional area of the petiole displays a rather
411 scattered association with LA (yet significant). In general, there is an allometric
412 relationship for deciduous species, whereas evergreen oaks are better adjusted to an
413 isometric scaling. As we first hypothesized, both hydraulic diameter and conductive area
414 scale with LA, either as a whole (A_c) or separating between xylem (A_x) and phloem (A_p).
415 This means that the larger the leaf, the greater the ability for bulk transport of water and
416 carbohydrates. Increasing the conductivity can be achieved either by increasing the
417 number of conduits, by producing wider conduits or by a combination of both strategies.
418 Nonetheless, the scaling becomes weaker in larger leaves.

419 The observed asymptotic response may reflect the different beforementioned constraints
420 that can compromise the functionality of the conducting tissues. The trade-off between
421 support and conduction functions of petioles could be explaining the constraint to produce
422 linearly larger conductive areas in larger leaves. The hydraulic diameter cannot scale
423 infinitely either. In the xylem, wider conduits are more susceptible to cavitation by both
424 drought and freezing. For phloem, leaves with wider sieve tube elements would require a
425 sugar production commensurate with the size of such conduits to generate an adequate
426 turgor pressure gradient to transport the phloem sap. Otherwise, allocation of sugars
427 would be hindered. Sieve elements differences can be found depending on the organ, age
428 and life-form. Thus, stems usually present the widest ones because of the presence of
429 secondary phloem, in contrast with organs with primary phloem such as leaves or petioles
430 (Woodruff, 2014; Prislán et al., 2019). Mature trees also present wider sieve elements
431 than seedlings or saplings (Kopanina et al., 2022). Finally, vines usually develop wider
432 sieve elements than free-standing plants, since they do not need as much support tissue
433 as a tree (Ewers and Fisher, 1991; Losada et al., 2022). Despite these differences,
434 interspecific variation of sieve element diameter is lower than for xylem vessel diameter,
435 which agrees with our results. Thus, the limitations imposed to phloem seem to be more

436 restrictive than those imposed to xylem. This makes sense if we consider that maintaining
437 the proper function of phloem is more critical than xylem for several reasons. First,
438 phloem sap flows during the whole day, night included, in contrast to xylem flow, which
439 reaches the highest values when stomata are opened during the day. Second, phloem must
440 maintain a constant turgor to achieve a steady flow since either an excessive viscosity or
441 a loss of turgor level will hinder the sap flow (Lang, 1978).

442 The scaling relationship between xylem and phloem areas has been also explored in
443 several studies (Table 5), which find an isometric scaling between A_x and A_p . Nonetheless,
444 most of these studies only focus on single species. Our work clearly improves this by
445 exploring the scaling relationship in a great number of species, closely related but
446 different enough in leaf habit and climatic ranges. Our data support an isometric scaling
447 in the case of deciduous species, but an allometric scaling between xylem and phloem in
448 evergreen species, favoring more production of xylem than phloem area (Fig. S1), which
449 reflects the higher values of XLA in evergreen species (see next section for further
450 details). A scaling relationship between the conductive areas in any case should be
451 expected, since both tissues are originated from the same meristematic tissue, i.e., the
452 procambium. In addition, despite having very different function, xylem and phloem are
453 interconnected. The main hydric relationship relies on xylem supplying water to load
454 phloem companion cells and sieve tubes according to a lateral water potential gradient
455 between both tissues. The flux of sugars depends on the product of water flux and sugar
456 concentration. Since the sugar concentration declines with distance from the leaf, water
457 flux must increase to keep the sap flux steady. In other words, there is an influx of water
458 from the xylem throughout the transport phloem to compensate for the lower sugar
459 concentrations. The balanced interaction between xylem and phloem is an essential
460 requirement for long-distance transport (Dinant and Lemoine, 2010; Sevanto, 2014).

461 Concerning the hydraulic conductivity after applying Hagen-Poiseuille law, we reported
462 an improvement in xylem K_h with LA, due to the combination of both a larger A_x and
463 wider d_h . This increment in xylem efficiency is still reflected even after removing the
464 effect of developing more A_x due to larger leaf areas, i.e., the K_{sx} . However, this is not the
465 case for phloem, where the dispersion of the data is much higher (Table 3). Here, solely
466 diameter of the phloem cells does not seem to predict the actual hydraulic conductivity
467 of phloem by itself, probably due to a mix of cellular types in the measurements. In
468 addition, some other factors related to the nature of sieve plates, such as the number of

469 pores, diameter of such pores and even number of plates per sieve element, are likely to
470 modulate the hydraulic conductivity of phloem.

471

472 *Deciduous and evergreen oaks follow different strategies producing and packaging their*
473 *conduits*

474 The main differences between deciduous and evergreen oak species arise when we
475 compare the conductive area standardized by LA (i.e., the XLA) with the K_{sx} and d_{hx} (Fig.
476 7). In this scenario, the range of variation in both K_{sx} and d_{hx} mainly corresponds with
477 deciduous species, whereas the range of variation in XLA mostly corresponds with
478 evergreen species. The larger LA of deciduous oaks requires a higher water supply which
479 is, in turn, reflected by a higher photosynthetic rate and stomatal conductance compared
480 to evergreen species. Thus, deciduous species display up to an order of magnitude higher
481 K_{sx} values than evergreen oaks. An increase in K_{sx} can be achieved either by reducing the
482 xylem area or by widening the xylem vessels for the same size and number of vessels,
483 which ultimately increases K_{hx} . Since the xylem area increases with LA, this increase in
484 K_{sx} in deciduous species can only be modulated by an increase in the diameter of the
485 xylem vessels. By contrast, evergreen oaks hardly present range of variation in their K_{sx}
486 values, with the exception of *Q. costaricensis*, the evergreen oak with the widest vessels
487 in this study.

488 Subsequently, we compared d_{hx} with XLA, but this time transforming K_{sx} into a more
489 physiologically meaningful variable, that is LSC, which links the capacity of xylem to
490 transport water with the leaf water demands (Mencuccini et al., 2019). In this correlation
491 (Fig. 7b), deciduous oaks always present low XLA values, close to or lower than one, but
492 they display a wide range of variation in their d_{hx} . Conversely, evergreen oaks exhibit a
493 wider variation in their XLA values but narrower d_{hx} values. In other words, deciduous
494 species tend to produce wider conduits to improve their xylem hydraulic conductivity for
495 a given leaf area, whereas evergreen species choose to increase their A_x for the same leaf
496 area over the d_h .

497 This dichotomous strategy between deciduous (Fig. 1, Model A) and evergreen (Fig. 1,
498 Model B) oaks could be directly related with both, their leaf life spans and the climatic
499 niches they occupy. First, deciduous leaves only have to keep functional for a few months
500 (typically 6-9 months). Thus, they can take a riskier but, simultaneously, a more effective

501 —showed by high LSC values— and a cheaper strategy (Ni et al., 2022). On the other
502 hand, evergreen species, whose leaves must remain productive for longer periods, tend to
503 follow a safer strategy at the expense of a more costly investment (Hacke et al., 2000).
504 Nonetheless, this investment in larger A_x also increases the LSC in those species with high
505 values of XLA, partly counterbalancing their lower K_{hx} values and reaching efficiencies
506 close to deciduous species. Besides, this safer strategy could be the main contributor to
507 the allometry found in xylem for evergreen species in comparison to the isometry that
508 most studies find and is also present in our deciduous species.

509 Second, deciduous oaks considered in this study are mainly represented by species
510 occupying temperate forests. These habitats rarely present stressful conditions (drought
511 and/or cold) during the lifespan of the leaves (Peguero-Pina et al., 2016). Hence, it is
512 reasonable to think that deciduous oaks could afford more efficient vessels at the expense
513 of more vulnerability. Accordingly, most of the evergreen oak species (with the exception
514 of some tropical ones; e.g., *Q. costaricensis*) must cope with at least one stressful period
515 during the year (typically a drought period), and even two in the case of Mediterranean
516 species (summer drought and winter cold) (Martín-Sánchez et al., 2022). Therefore, it is
517 justifiable to consider that these species choose a conservative strategy for building their
518 conductive tissues. Furthermore, deciduous oaks occupying extra-temperate habitats with
519 stressful periods such as the Mediterranean Basin (e.g., *Q. faginea* and *Q. ithaburensis*)
520 or winter-dry temperate climates in Mexico (e.g., *Q. crassipes*) present the smallest values
521 of both leaf area and hydraulic diameter among deciduous oaks, suggesting the reduction
522 of xylem vessels in environmental restrictive habitats. Indeed, aridity index shows
523 correlation with d_{hx} for both deciduous and evergreen species. The more xeric the climate
524 is, the narrower the xylem vessels are. This relationship between drought and vessel size
525 has been widely reported by numerous authors in stems, branches and leaves, resulting in
526 a trade-off between efficiency and safety (Hajek et al., 2014; Pivovarovoff et al., 2016;
527 Schreibet et al., 2016; Barotto et al., 2017). It has also been recently found in petioles by
528 comparing XLA and resistance to cavitation in several *Eucalyptus* species (Blackman et
529 al., 2023). Likewise, this compensation of improving the hydraulic conductivity by
530 increasing the conductive area over the diameters of the conduits has been also reported
531 in stems of several species (Nardini et al., 2012) but, to our knowledge, it has never been
532 attributed to leaf habit in any case.

533 We demonstrate the presence of two models for producing and packaging the conduits,
534 and we also prove the relationship between aridity and hydraulic diameter. However, we
535 did not find significant correlation between cold, here represented by the WorldClim2
536 variable “mean of daily minimum temperatures during the coldest quarter”, and d_{hx} in
537 evergreen oaks. Nonetheless, cavitation induced by winter cold is caused by freeze-thaw
538 cycles, a climatic variable for which global-scale data are not available. The lack of
539 significance is mainly due to two species: *Q. semecarpifolia* and *Q. engleriana*. These
540 evergreen species present a wide range of distribution in Asia, in habitats that present a
541 complex orography, resulting in very different climatic conditions. A detailed study in
542 their natural habitats along altitudinal and climatic gradients, measuring the daily
543 temperatures, might reveal a reduction in d_{hx} in those sites where trees have to withstand
544 more frequent freeze-thaw cycles. Other species, such as *Q. chrysolepis* and *Q.*
545 *monimotricha*, for instance, the two species with the narrowest vessels, can be found in
546 very high-altitude habitats, where they are exposed to recurrent frosts during the coldest
547 months. Thus, according to the leaf economic spectrum, these species would not recover
548 the investment in case such expensive leaves died earlier due to a hydraulic failure. By
549 contrast, evergreen species with the widest vessels (e.g. *Q. costaricensis*, *Q. virginiana*)
550 occupy tropical or subtropical habitats with the absence of strong and frequent frosts.

551

552 *Anatomy of petioles accommodates physiological demands*

553 Our data supports a strong correlation between the petiole anatomical traits of both, xylem
554 and phloem, and the estimated g_s and A_N at leaf-level. The strongest relationships are
555 found between xylem traits and $A_{N,leaf}$, albeit xylem- $g_{s,leaf}$ correlations shows similar
556 statistical power. Even though Figures 8 and 9 represent deciduous and evergreen species
557 in different colours, the aim is not to see differences in leaf habit but explore the
558 anatomical architecture in response to the physiological demands of the leaf lamina. This
559 link function-structure has been proposed to be mediated throughout several
560 physiological processes, such as water potential, hydraulic conductance, turgor pressure
561 or sugar concentration (Hölttä et al., 2010). These factors would have an effect on the
562 ontogeny and development of the cells in a tissue (Cosgrove, 1993).

563 Relationships between xylem area in the petiole and leaf transpiration were proposed
564 more than one hundred years ago by Salisbury (1913). However, this author suggested

565 that the nature of the conduits —i.e., number and size— should receive more attention.
566 Here, we explore not only such relationship between A_x and $g_{s,leaf}$, but also the size of the
567 conduits and the calculated K_{hx} , which all resulted to be highly correlated with $g_{s,leaf}$.
568 Brocious and Hacke (2016), presented a study among different *Populus* hybrids where no
569 differences among several clones were found, however, when all leaves were analyzed
570 together, they found similar trends to our findings for A_x and K_{hx} in relation to g_s ,
571 suggesting that ‘lamina size is constrained by the transport capacity of the vascular tissue
572 in the petiole’. Concerning the scaling relationship, our results show an allometry in all
573 cases. In this regard, Zhong et al. (2020) also found allometric scaling in 53 woody
574 species between xylem area in the midrib and the number of stomata in the leaf lamina,
575 but they reported an isometric scaling of leaf area and total stomatal area. Nonetheless, it
576 must not be disregarded that stomatal conductance is only showing the capacity of
577 stomata to release water to atmosphere, but the transpiration rate is the variable actually
578 measuring water losses in leaves by taking into account the vapor pressure deficit (VPD).
579 In this context, part of the scatter observed in the association between petiole xylem traits
580 and $g_{s,leaf}$ might be attributed to adaptations to different VPD levels during the growing
581 season.

582 A higher photosynthetic rate is related to a larger xylem hydraulic conductance because
583 of a greater water usage (Brodribb and Field, 2000; Hölttä et al., 2010). The largest leaves
584 among our species correspond with deciduous species, and they present a higher $A_{N,leaf}$
585 compared to evergreen species. However, when A_N —expressed in m^2 — is compared, no
586 significant differences linked to leaf habit are found (Peguero-Pina et al., 2017). In this
587 case, taking into account the total photosynthesis rate at leaf level is more logical than
588 standardizing it for a given area because a petiole must have an anatomical structure able
589 to export the sucrose produced by the leaf. Sucrose is the most abundant photosynthate
590 transported by sieve elements, but viscosity of a sucrose solution increases exponentially
591 with increasing concentration (Morison, 2002). Furthermore, the viscosity of the sap is
592 one of the main factors that limit phloem transport, since the more viscous the solution,
593 the lower the flow rate (Lang, 1978; Sevanto, 2014). To deal with this disadvantage, plants
594 can choose between two strategies. On the one hand, sink organs could lower their sugar
595 concentration, increasing the source-sink concentration gradient. On the other hand, they
596 could develop wider sieve tubes, since an increment in the radius of a sieve tube should
597 improve the hydraulic conductivity to the fourth power. This latter strategy seems to be

598 more feasible for the plant (Hölttä et al., 2009; Sevanto, 2014). Thus, the largest leaves in
599 oak species, which are in turn the ones which produce more sucrose, would need wider
600 sieve tubes to avoid a depleted flow rate caused by an excessive viscosity.

601

602 CONCLUSION

603 The conductive tissues in the petiole scale allometrically with leaf area, which ultimately
604 reflects the demands on the leaf. Xylem and phloem present a very similar pattern in their
605 scaling both for conductive areas and for the diameters of their cells. Although increasing
606 the diameter of the conduits would imply a greater improvement in the hydraulic
607 conductivity than increasing the conductive area, it also results in a riskier strategy. For
608 this reason, a coordinated scaling between both alternatives is required depending on the
609 habitat occupied by the species. For example, species inhabiting arid habitats tend to have
610 narrower conduits than those species occupying cool nemoral habitats.

611 We find that oaks with different leaf habits tend to improve their hydraulic conductivities
612 with two contrasting approaches. Deciduous species opt to produce wider vessels for the
613 same conductive and leaf areas compared to evergreen oaks. Conversely, evergreen
614 species choose to increase their conductive area over the diameter of the conduits.

615 Most studies inquiring into the scaling between xylem and phloem find isometric
616 relationships. Deciduous oaks exhibit the same isometric pattern. However, evergreen
617 species present an allometric scaling, producing more xylem than phloem, which agrees
618 with their safer strategy.

619 Phloem is more constrained than xylem in increasing the diameter of its main conduits.
620 This is probably related to the very different functionality of both tissues. While xylem
621 mainly responds to water demands during the photosynthesis, phloem is responsible for
622 maintaining a proper balance of sugars, hormones and other metabolites throughout the
623 plant and throughout the day.

624 The structure of the conductive tissues straightly corresponds with leaf demands. Xylem
625 area, vessel size and hydraulic conductivity in the petiole are correlated with both
626 photosynthesis net rate and stomatal conductance at leaf level. Phloem anatomy also
627 relates to photosynthesis rate.

628

629 ACKNOWLEDGEMENTS

630 We thank Jardín Botánico de Iturrarán and Francisco Garín for allowing us to collect oak
631 leaf samples from their garden. This research was supported by Grant PID2022-
632 136478OB-C32 funded by MICIU/AEI/10.13039/501100011033 and by “ERDF A way
633 of making Europe”, by grant CNS2022-136156 funded by
634 MCIN/AEI/10.13039/501100011033 and European Union Next Generation EU/PRTR
635 and by Gobierno de Aragón S74_23R research group. The work of Rubén Martín-
636 Sánchez was supported by a PhD Gobierno de Aragón scholarship.

637

638 DATA AVAILABILITY STATEMENT

639 The data that supports the findings of this study are available in
640 <https://doi.org/https://doi.org/10.5281/zenodo.12730852>.

641 REFERENCES

- 642 1. Alonso-Forn, D., Sancho-Knapik, D., Ferrio, J. P., Peguero-Pina, J. J., Bueno,
643 A., Onoda, Y., Cavender-bares, J., Niinemets, Ü., Jansen, S., Riederer, M.,
644 Cornelissen, J.H.C., Chai, Y., & Gil-Pelegrín, E. (2020). Revisiting the
645 functional basis of sclerophylly within the leaf economics spectrum of oaks:
646 different roads to Rome. *Current Forestry Reports*, 6(4), 260-281.
647 <https://doi.org/10.1007/s40725-020-00122-7>.
- 648 2. Alonso-Forn, D., Peguero-Pina, J. J., Ferrio, J. P., Mencuccini, M., Mendoza-
649 Herrer, Ó., Sancho-Knapik, D., & Gil-Pelegrín, E. (2021). Contrasting
650 functional strategies following severe drought in two Mediterranean oaks with
651 different leaf habit: *Quercus faginea* and *Quercus ilex* subsp. *rotundifolia*. *Tree*
652 *Physiology*, 41(3), 371-387. <https://doi.org/10.1093/treephys/tpaa135>.
- 653 3. Barotto, A. J., Monteoliva, S., Gyenge, J., Martinez-Meier, A., & Fernandez,
654 M. E. (2018). Functional relationships between wood structure and
655 vulnerability to xylem cavitation in races of *Eucalyptus globulus* differing in
656 wood density. *Tree Physiology*, 38(2), 243-251.
657 <https://doi.org/10.1093/treephys/tpx138>.
- 658 4. Blackman, C. J., Halliwell, B., Hartill, G. E., & Brodribb, T. J. (2024). Petiole
659 XLA (xylem to leaf area ratio) integrates hydraulic safety and efficiency across
660 a diverse group of eucalypt leaves. *Plant, Cell & Environment*, 47(1), 49-58.
661 <https://doi.org/10.1111/pce.14713>.
- 662 5. Brocious, C. A., & Hacke, U. G. (2016). Stomatal conductance scales with
663 petiole xylem traits in *Populus* genotypes. *Functional Plant Biology*, 43(6),
664 553-562. <https://doi.org/10.1071/FP15336>.
- 665 6. Brodribb, T. J., & Feild, T. S. (2000). Stem hydraulic supply is linked to leaf
666 photosynthetic capacity: evidence from New Caledonian and Tasmanian
667 rainforests. *Plant, Cell & Environment*, 23(12), 1381-1388.
668 <https://doi.org/10.1046/j.1365-3040.2000.00647.x>.
- 669 7. Cai, J., & Tyree, M. T. (2010). The impact of vessel size on vulnerability
670 curves: data and models for within-species variability in saplings of aspen,
671 *Populus tremuloides* Michx. *Plant, Cell & Environment*, 33(7), 1059-1069.
672 <https://doi.org/10.1111/j.1365-3040.2010.02127.x>.

- 673 8. Carvalho, M. R., Turgeon, R., Owens, T., & Niklas, K. J. (2017a). The scaling
674 of the hydraulic architecture in poplar leaves. *New Phytologist*, 214(1), 145-
675 157. <https://doi.org/10.1111/nph.14385>.
- 676 9. Carvalho, M. R., Turgeon, R., Owens, T., & Niklas, K. J. (2017b). The
677 hydraulic architecture of Ginkgo leaves. *American Journal of Botany*, 104(9),
678 1285-1298. <https://doi.org/10.3732/ajb.1700277>.
- 679 10. Cochard, H., & Tyree, M. T. (1990). Xylem dysfunction in *Quercus*: vessel
680 sizes, tyloses, cavitation and seasonal changes in embolism. *Tree physiology*,
681 6(4), 393-407. <https://doi.org/10.1093/treephys/6.4.393>.
- 682 11. Cosgrove, D. J. (1993). Wall extensibility: its nature, measurement and
683 relationship to plant cell growth. *New Phytologist*, 124(1), 1-23.
684 <https://doi.org/10.1111/j.1469-8137.1993.tb03795.x>.
- 685 12. Dinant, S., & Lemoine, R. (2010). The phloem pathway: new issues and old
686 debates. *Comptes Rendus Biologies*, 333(4), 307-319.
687 <https://doi.org/10.1071/PP9780535>.
- 688 13. Esau, K. (1939). Development and structure of the phloem tissue. *The*
689 *Botanical Review*, 5, 373-432. <https://doi.org/10.1007/BF02878295>.
- 690 14. Ewers, F. W., & Fisher, J. B. (1991). Why vines have narrow stems:
691 histological trends in *Bauhinia* (Fabaceae). *Oecologia*, 88, 233-237.
692 <https://doi.org/10.1007/BF00320816>.
- 693 15. Fick, S.E. & R.J. Hijmans, (2017). WorldClim 2: new 1km spatial resolution
694 climate surfaces for global land areas. *International Journal of Climatology*,
695 37 (12), 4302-4315.
- 696 16. Gil-Pelegrín, E., Saz, M.Á., Cuadrat, J.M., Peguero-Pina, J.J., Sancho-Knapik,
697 D. (2017). Oaks Under Mediterranean-Type Climates: Functional Response to
698 Summer Aridity. In: Gil-Pelegrín, E., Peguero-Pina, J., Sancho-Knapik, D.
699 (eds) *Oaks Physiological Ecology. Exploring the Functional Diversity of*
700 *Genus Quercus L.. Tree Physiology*, vol 7. Springer, Cham.
701 https://doi.org/10.1007/978-3-319-69099-5_5.
- 702 17. Giordano, R., Salleo, A., Salleo, S., & Wanderlingh, F. (1978). Flow in xylem
703 vessels and Poiseuille's law. *Canadian Journal of Botany*, 56(3), 333-338.
704 <https://doi.org/10.1139/b78-039>.
- 705 18. Gleason, S. M., Blackman, C. J., Chang, Y., Cook, A. M., Laws, C. A., &
706 Westoby, M. (2016). Weak coordination among petiole, leaf, vein, and gas-

- 707 exchange traits across Australian angiosperm species and its possible
708 implications. *Ecology and Evolution*, 6(1), 267-278.
709 <https://doi.org/10.1002/ece3.1860>.
- 710 19. Hacke, U., & Sauter, J. J. (1996). Drought-induced xylem dysfunction in
711 petioles, branches, and roots of *Populus balsamifera* L. and *Alnus glutinosa*
712 (L.) Gaertn. *Plant Physiology*, 111(2), 413-417.
713 <https://doi.org/10.1104/pp.111.2.413>
- 714 20. Hacke, U. G., Sperry, J. S., & Pittermann, J. (2000). Drought experience and
715 cavitation resistance in six shrubs from the Great Basin, Utah. *Basic and*
716 *Applied Ecology*, 1(1), 31-41. <https://doi.org/10.1078/1439-1791-00006>.
- 717 21. Hacke, U. G., Sperry, J. S., Wheeler, J. K., & Castro, L. (2006). Scaling of
718 angiosperm xylem structure with safety and efficiency. *Tree physiology*, 26(6),
719 689-701. <https://doi.org/10.1093/treephys/26.6.689>.
- 720 22. Hajek, P., Leuschner, C., Hertel, D., Delzon, S., & Schuldt, B. (2014). Trade-
721 offs between xylem hydraulic properties, wood anatomy and yield in *Populus*.
722 *Tree physiology*, 34(7), 744-756. <https://doi.org/10.1093/treephys/tpu048>.
- 723 23. Harayama, H., Ishida, A., & Yoshimura, J. (2016). Overwintering evergreen
724 oaks reverse typical relationships between leaf traits in a species spectrum.
725 *Royal Society Open Science*, 3(7), 160276.
726 <https://doi.org/10.1098/rsos.160276>.
- 727 24. Hartig F. (2022). DHARMa: Residual Diagnostics for Hierarchical (Multi-
728 Level / Mixed) Regression Models. R package version 0.4.6. [https://cran.r-](https://cran.r-project.org/web/packages/DHARMa)
729 [project.org/web/packages/DHARMa](https://cran.r-project.org/web/packages/DHARMa).
- 730 25. Hirose, S., Kume, A., Takeuchi, S., Utsumi, Y., Otsuki, K., & Ogawa, S.
731 (2005). Stem water transport of *Lithocarpus edulis*, an evergreen oak with
732 radial-porous wood. *Tree physiology*, 25(2), 221-
733 228. <https://doi.org/10.1093/treephys/25.2.221>.
- 734 26. Hölttä, T., Mäkinen, H., Nöjd, P., Mäkelä, A., & Nikinmaa, E. (2010). A
735 physiological model of softwood cambial growth. *Tree Physiology*, 30(10),
736 1235-1252. <https://doi.org/10.1093/treephys/tpq068>.
- 737 27. Hölttä, T., Mencuccini, M., & Nikinmaa, E. (2009). Linking phloem function
738 to structure: analysis with a coupled xylem–phloem transport model. *Journal*
739 *of theoretical biology*, 259(2), 325-337.
740 <https://doi.org/10.1016/j.jtbi.2009.03.039>.

- 741 28. Huang, W., Hu, H., & Zhang, S. B. (2016). Photosynthesis and photosynthetic
742 electron flow in the alpine evergreen species *Quercus guyavifolia* in winter.
743 *Frontiers in Plant Science*, 7, 204522.
744 <https://doi.org/10.3389/fpls.2016.01511>.
- 745 29. Jacobsen, A. L., Pratt, R. B., Venturas, M. D., & Hacke, U. G. (2019). Large
746 volume vessels are vulnerable to water-stress-induced embolism in stems of
747 poplar. *IAWA journal*, 40(1), 4-S4. [https://doi.org/10.1163/22941932-](https://doi.org/10.1163/22941932-40190233)
748 [40190233](https://doi.org/10.1163/22941932-40190233).
- 749 30. Jafarnia, S., Akbarinia, M., Hosseinpour, B., Modarres Sanavi, S. A. M., &
750 Salami, S. A. (2018). Effect of drought stress on some growth, morphological,
751 physiological, and biochemical parameters of two different populations of
752 *Quercus brantii*. *iForest-Biogeosciences and Forestry*, 11(2), 212.
753 <https://doi.org/10.3832/ifor2496-010>.
- 754 31. Jensen, K. H., Savage, J. A., & Holbrook, N. M. (2013). Optimal concentration
755 for sugar transport in plants. *Journal of the Royal Society Interface*, 10(83),
756 20130055. <https://doi.org/10.1098/rsif.2013.0055>.
- 757 32. Jyske, T., & Hölttä, T. (2015). Comparison of phloem and xylem hydraulic
758 architecture in *Picea abies* stems. *New phytologist*, 205(1), 102-115.
759 <https://doi.org/10.1111/nph.12973>.
- 760 33. Kar, S., Montague, D. T., & Villanueva-Morales, A. (2021). Measurement of
761 photosynthesis in excised leaves of ornamental trees: a novel method to
762 estimate leaf level drought tolerance and increase experimental sample size.
763 *Trees*, 35, 889-905. [10.1111/j.2041-210X.2011.00153.x](https://doi.org/10.1111/j.2041-210X.2011.00153.x)
764 [10.1007/s00468-021-02088-w](https://doi.org/10.1111/j.2041-210X.2011.00153.x).
- 765 34. Kikuzawa, K., Onoda, Y., Wright, I. J., & Reich, P. B. (2013). Mechanisms
766 underlying global temperature-related patterns in leaf longevity. *Global
767 Ecology and Biogeography*, 22(8), 982-993.
768 <https://doi.org/10.1111/geb.12042>.
- 769 35. Kiorapostolou, N., & Petit, G. (2019). Similarities and differences in the
770 balances between leaf, xylem and phloem structures in *Fraxinus ornus* along
771 an environmental gradient. *Tree Physiology*, 39(2), 234-242.
772 <https://doi.org/10.1093/treephys/tpy095>.
- 773 36. Kopanina, A. V., Talskikh, A. I., Vlasova, I. I., & Kotina, E. L. (2022). Age-
774 related pattern in bark formation of *Betula ermanii* growing in volcanic

- 775 environments from southern Sakhalin and Kuril Islands (Northeast Asia).
776 *Trees*, 36(3), 915-939. <https://doi.org/10.1007/s00468-021-02257-x>.
- 777 37. Lang, A. (1978). A model of mass flow in the phloem. *Functional Plant*
778 *Biology*, 5(4), 535-546. <https://doi.org/10.1071/PP9780535>.
- 779 38. Lemoine, D., Granier, A., & Cochard, H. (1999). Mechanism of freeze-
780 induced embolism in *Fagus sylvatica* L. *Trees*, 13, 206-210.
781 <https://doi.org/10.1007/PL00009751>.
- 782 39. Llusia, J., Roahtyn, S., Yakir, D., Rotenberg, E., Seco, R., Guenther, A., &
783 Penuelas, J. (2016). Photosynthesis, stomatal conductance and terpene
784 emission response to water availability in dry and mesic Mediterranean
785 forests. *Trees*, 30, 749-759. <https://doi.org/10.1007/s00468-015-1317-x>.
- 786 40. Lo Gullo, M. A., & Salleo, S. (1993). Different vulnerabilities of *Quercus ilex*
787 L. to freeze-and summer drought-induced xylem embolism: an ecological
788 interpretation. *Plant, Cell & Environment*, 16(5), 511-519.
789 <https://doi.org/10.1111/j.1365-3040.1993.tb00898.x>.
- 790 41. Losada, J. M., He, Z., & Holbrook, N. M. (2022). Sieve tube structural
791 variation in *Austrobaileya scandens* and its significance for lianescence. *Plant,*
792 *Cell & Environment*, 45(8), 2460-2475. <https://doi.org/10.1111/pce.14361>.
- 793 42. Martín-Sánchez, R., Peguero-Pina, J. J., Alonso-Forn, D., Ferrio, J. P., Sancho-
794 Knapik, D., & Gil-Peigrín, E. (2022). Summer and winter can equally stress
795 holm oak (*Quercus ilex* L.) in Mediterranean areas: a physiological view.
796 *Flora*, 290, 152058. <https://doi.org/10.1016/j.flora.2022.152058>.
- 797 43. Martín-Sánchez, R., Sancho-Knapik, D., Alonso-Forn, D., López-Ballesteros,
798 A., Ferrio, J. P., Hipp, A. L., Peguero-Pina, J.J., & Gil-Peigrín, E. (2024). Oak
799 leaf morphology may be more strongly shaped by climate than by phylogeny.
800 *Annals of Forest Science*, 81(1), 14. [https://doi.org/10.1186/s13595-024-](https://doi.org/10.1186/s13595-024-01232-z)
801 [01232-z](https://doi.org/10.1186/s13595-024-01232-z).
- 802 44. Mediavilla, S., García-Ciudad, A., García-Criado, B., & Escudero, A. (2008).
803 Testing the correlations between leaf life span and leaf structural
804 reinforcement in 13 species of European Mediterranean woody plants.
805 *Functional Ecology*, 22(5), 787-793. [https://doi.org/10.1111/j.1365-](https://doi.org/10.1111/j.1365-2435.2008.01453.x)
806 [2435.2008.01453.x](https://doi.org/10.1111/j.1365-2435.2008.01453.x).
- 807 45. Mencuccini, M., Rosas, T., Rowland, L., Choat, B., Cornelissen, H., Jansen,
808 S., ... & Martínez-Vilalta, J. (2019). Leaf economics and plant hydraulics drive

- 809 leaf: wood area ratios. *New Phytologist*, 224(4), 1544-1556.
810 <https://doi.org/10.1111/nph.15998>.
- 811 46. Morison, K. R. (2002). Viscosity equations for sucrose solutions: old and new
812 2002. In *Proceedings of the 9th APCChE Congress and CHEMECA*.
- 813 47. Nagel, J. M., Griffin, K. L., Schuster, W. S., Tissue, D. T., Turnbull, M. H.,
814 Brown, K. J., & Whitehead, D. (2002). Energy investment in leaves of red
815 maple and co-occurring oaks within a forested watershed. *Tree Physiology*,
816 22(12), 859-867. <https://doi.org/10.1093/treephys/22.12.859>.
- 817 48. Nardini, A., Pedà, G., & La Rocca, N. (2012). Trade-offs between leaf
818 hydraulic capacity and drought vulnerability: morpho-anatomical bases,
819 carbon costs and ecological consequences. *New Phytologist*, 196(3), 788-798.
820 <https://doi.org/10.1111/j.1469-8137.2012.04294.x>.
- 821 49. Ni, X., Sun, L., Cai, Q., Ma, S., Feng, Y., Sun, Y., An, L., & Ji, C. (2022).
822 Variation and determinants of leaf anatomical traits from boreal to tropical
823 forests in eastern China. *Ecological Indicators*, 140, 108992.
824 <https://doi.org/10.1016/j.ecolind.2022.108992>.
- 825 50. Peguero-Pina, J. J., Sancho-Knapik, D., Martín, P., Saz, M. Á., Gea-Izquierdo,
826 G., Cañellas, I., & Gil-Pelegrín, E. (2015). Evidence of vulnerability
827 segmentation in a deciduous Mediterranean oak (*Quercus subpyrenaica* EH
828 del Villar). *Trees*, 29, 1917-1927. <https://doi.org/10.1007/s00468-015-1273-5>.
- 829 51. Peguero-Pina, J. J., Sisó, S., Sancho-Knapik, D., Díaz-Espejo, A., Flexas, J.,
830 Galmés, J., & Gil-Pelegrín, E. (2016). Leaf morphological and physiological
831 adaptations of a deciduous oak (*Quercus faginea* Lam.) to the Mediterranean
832 climate: a comparison with a closely related temperate species (*Quercus robur*
833 L.). *Tree Physiology*, 36(3), 287-299. <https://doi.org/10.1093/treephys/tpv107>.
- 834 52. Peguero-Pina, J. J., Aranda, I., Cano, F. J., Galmés, J., Gil-Pelegrín, E.,
835 Niinemets, Ü., Sancho-Knapik, D., & Flexas, J. (2017). The role of mesophyll
836 conductance in oak photosynthesis: among-and within-species variability. In:
837 Gil-Pelegrín, E., Peguero-Pina, J., Sancho-Knapik, D. (eds) *Oaks*
838 *Physiological Ecology. Exploring the Functional Diversity of Genus Quercus*
839 L.. *Tree Physiology*, vol 7. Springer, Cham. https://doi.org/10.1007/978-3-319-69099-5_9.
- 841 53. Peguero-Pina, J. J., Vilagrosa, A., Alonso-Forn, D., Ferrio, J. P., Sancho-
842 Knapik, D., & Gil-Pelegrín, E. (2020). Living in drylands: Functional

- 843 adaptations of trees and shrubs to cope with high temperatures and water
844 scarcity. *Forests*, 11(10), 1028. <https://doi.org/10.3390/f11101028>.
- 845 54. Pivovarov, A. L., Pasquini, S. C., De Guzman, M. E., Alstad, K. P., Stemke,
846 J. S., & Santiago, L. S. (2016). Multiple strategies for drought survival among
847 woody plant species. *Functional Ecology*, 30(4), 517-526.
848 <https://doi.org/10.1111/1365-2435.12518>.
- 849 55. Prislán, P., Mrak, P., Žnidaršič, N., Štrus, J., Humar, M., Thaler, N., Mrak, T.,
850 & Gričar, J. (2019). Intra-annual dynamics of phloem formation and
851 ultrastructural changes in sieve tubes in *Fagus sylvatica*. *Tree Physiology*,
852 39(2), 262-274. <https://doi.org/10.1093/treephys/tpy102>.
- 853 56. Ray, D. M., & Jones, C. S. (2018). Scaling relationships and vessel packing in
854 petioles. *American Journal of Botany*, 105(4), 667-676.
855 <https://doi.org/10.1002/ajb2.1054>.
- 856 57. Salisbury, E. J. (1913). The determining factors in petiolar structure. *New*
857 *Phytologist*, 12(8), 281-289.
- 858 58. Sancho-Knapik, D., Escudero, A., Mediavilla, S., Scoffoni, C., Zailaa, J.,
859 Cavender-Bares, J., Álvarez-Arenas, T.G., Molins, A., Alonso-Forn, D.,
860 Ferrio, J.P., Peguero-Pina, J.J., & Gil-Pelegrín, E. (2021). Deciduous and
861 evergreen oaks show contrasting adaptive responses in leaf mass per area
862 across environments. *New Phytologist*, 230(2), 521-534.
863 <https://doi.org/10.1111/nph.17151>.
- 864 59. Schreiber, S. G., Hacke, U. G., Chamberland, S., Lowe, C. W., Kamelchuk,
865 D., Bräutigam, K., ... & Thomas, B. R. (2016). Leaf size serves as a proxy for
866 xylem vulnerability to cavitation in plantation trees. *Plant, Cell &*
867 *Environment*, 39(2), 272-281. <https://doi.org/10.1111/pce.12611>.
- 868 60. Sevanto, S. (2014). Phloem transport and drought. *Journal of experimental*
869 *botany*, 65(7), 1751-1759. <https://doi.org/10.1093/jxb/ert467>.
- 870 61. Sevanto, S., Holbrook, N. M., & Ball, M. C. (2012). Freeze/thaw-induced
871 embolism: probability of critical bubble formation depends on speed of ice
872 formation. *Frontiers in Plant Science*, 3, 107.
873 <https://doi.org/10.3389/fpls.2012.00107>.
- 874 62. Sperry, J. S., & Sullivan, J. E. (1992). Xylem embolism in response to freeze-
875 thaw cycles and water stress in ring-porous, diffuse-porous, and conifer

- 876 species. *Plant physiology*, 100(2), 605-613.
877 <https://doi.org/10.1104/pp.100.2.605>.
- 878 63. Sperry, J. S., Nichols, K. L., Sullivan, J. E., & Eastlack, S. E. (1994). Xylem
879 embolism in ring-porous, diffuse-porous, and coniferous trees of northern
880 Utah and interior Alaska. *Ecology*, 75(6), 1736-1752.
881 <https://doi.org/10.2307/1939633>.
- 882 64. Thadani, R., Berlyn, G. P., & Ashton, M. S. (2009). A comparison of leaf
883 physiology and anatomy of two Himalayan oaks in response to different light
884 environments. *Journal of sustainable forestry*, 28(1-2), 74-91.
885 <https://doi.org/10.1080/10549810802626159>.
- 886 65. Thompson, M. V. (2006). Phloem: the long and the short of it. *Trends in plant*
887 *science*, 11(1), 26-32.
- 888 66. Tyree, M. T. (2003). Hydraulic limits on tree performance: transpiration,
889 carbon gain and growth of trees. *Trees*, 17, 95-100.
890 <https://doi.org/10.1007/s00468-002-0227-x>.
- 891 67. Tyree, M. T., & Sperry, J. S. (1989). Vulnerability of xylem to cavitation and
892 embolism. *Annual review of plant biology*, 40(1), 19-36.
893 <https://doi.org/10.1146/annurev.pp.40.060189.000315>.
- 894 68. Tyree, M.T., & Zimmermann, M.H. (2002). Hydraulic Architecture of Whole
895 Plants and Plant Performance. In: *Xylem Structure and the Ascent of Sap*.
896 Springer Series in Wood Science. Springer, Berlin, Heidelberg.
897 https://doi.org/10.1007/978-3-662-04931-0_6
- 898 69. Vaitkus, M. R., & McLeod, K. W. (1995). Photosynthesis and water-use
899 efficiency of two sandhill oaks following additions of water and nutrients.
900 *Bulletin of the Torrey Botanical Club*, 30-39.
901 <https://doi.org/10.2307/2996401>.
- 902 70. Vignali, S., Barras, A. G., Arlettaz, R., & Braunisch, V. (2020). SDMtune: An
903 R package to tune and evaluate species distribution models. *Ecology and*
904 *Evolution*, 10(20), 11488-11506. <https://doi.org/10.1002/ece3.6786>.
- 905 71. Warton, D. I., Duursma, R. A., Falster, D. S., & Taskinen, S. (2012). smatr 3–
906 an R package for estimation and inference about allometric lines. *Methods in*
907 *ecology and evolution*, 3(2), 257-259. [https://doi.org/10.1111/j.2041-](https://doi.org/10.1111/j.2041-210X.2011.00153.x)
908 [210X.2011.00153.x](https://doi.org/10.1111/j.2041-210X.2011.00153.x).

- 909 72. West, G. B., Brown, J. H., & Enquist, B. J. (1997). A general model for the
910 origin of allometric scaling laws in biology. *Science*, 276(5309), 122-126.
911 <https://doi.org/10.1126/science.276.5309.122>.
- 912 73. Will, T., & van Bel, A. J. (2006). Physical and chemical interactions between
913 aphids and plants. *Journal of experimental botany*, 57(4), 729-737.
914 <https://doi.org/10.1093/jxb/erj089>.
- 915 74. Will, T., Furch, A. C., & Zimmermann, M. R. (2013). How phloem-feeding
916 insects face the challenge of phloem-located defenses. *Frontiers in plant
917 science*, 4, 336.<https://doi.org/10.3389/fpls.2013.00336>.
- 918 75. Woodruff, D. R. (2014). The impacts of water stress on phloem transport in
919 Douglas-fir trees. *Tree physiology*, 34(1), 5-14.
920 <https://doi.org/10.1093/treephys/tpt106>.
- 921 76. Zanne, A.E., Tank, D.C., Cornwell, W.K., Eastman, J.M., Smith, S.A.,
922 FitzJohn, R.G., McGlinn, D.J., O'Meara, B.C., Moles, A.T., Reich, P.B.,
923 Royer, D.L., Soltis, D.E., Stevens, P.F., Westoby, M., Wright, I.J., Aarssen, L.,
924 Bertin, R.I., Calaminus, A., Govaerts, R., Hemmings, F., Leishman, M.R.,
925 Oleksyn, J., Soltis, P.S., Swenson, N.G., Warman, L., Beaulieu, J.M. (2014).
926 Three keys to the radiation of angiosperms into freezing environments. *Nature*
927 514, 394. <https://doi.org/10.1038/nature13842>.
- 928 77. Zhong, M., Cerabolini, B. E., Castro-Díez, P., Puyravaud, J. P., & Cornelissen,
929 J. H. (2020). Allometric co-variation of xylem and stomata across diverse
930 woody seedlings. *Plant, Cell & Environment*, 43(9), 2301-2310.
931 <https://doi.org/10.1111/pce.13826>.
- 932 78. Zwieniecki, M. A., Melcher, P. J., Feild, T. S., & Holbrook, N. M. (2004). A
933 potential role for xylem–phloem interactions in the hydraulic architecture of
934 trees: effects of phloem girdling on xylem hydraulic conductance. *Tree
935 Physiology*, 24(8), 911-917. <https://doi.org/10.1093/treephys/24.8.911>.

937 **TABLES**938 **Table 1.** Appendix of traits measured in this study; their abbreviations and units.

Parameter	Abbreviation	Unit
Leaf Area	LA	cm ²
Petiole area	A_{pet}	μm ²
Conductive area	A_c	μm ²
Xylem area	A_x	μm ²
Hydraulic diameter of xylem	d_{hx}	μm
Ratio xylem area/leaf area	XLA	cm ² m ⁻²
Hydraulic conductivity of xylem	K_{hx}	Kg m Mpa ⁻¹ s ⁻¹
Specific conductivity of xylem	K_{sx}	Kg m ⁻¹ Mpa ⁻¹ s ⁻¹
Phloem area	A_p	μm ²
Hydraulic diameter of phloem	d_{hp}	μm
Ratio phloem area/leaf area	PLA	cm ² m ⁻²
Hydraulic conductivity of phloem	K_{hp}	Kg m Mpa ⁻¹ s ⁻¹
Photosynthesis net assimilation per leaf	A_{N,leaf}	μmol CO ₂ s ⁻¹
Stomatal conductance per leaf	g_{s,leaf}	mmol H ₂ O s ⁻¹
Mean annual temperature	MAT	°C
Mean annual precipitation	MAP	mm
Mean of daily minimum temperatures during the coldest quarter	T_{min}	°C
Aridity Index	AI	Dimensionless

939

940 **Table 2.** Percentage of variance explained by leaf habit (deciduous and evergreen)
 941 according to the ANOVA performed for each trait measured individually. Leaf traits
 942 notation as in Table 1. Significance level is showed with asterisks (*** < 0.001, ** =
 943 0.001-0.01, * = 0.01-0.05, n.s. > 0.05).

Trait	Leaf Habit	Residuals
LA	37.43 ***	62.57
A_{pet}	5.4 n.s.	94.6
A_c	14.12 *	85.88
A_x	13.97 ***	86.03
d_{hx}	32.51 ***	67.49
XLA	32.95 ***	67.05
K_{hx}	18.22 ***	81.78
K_{sx}	28.61 ***	71.39
A_p	11.72 ***	88.28

d_{hp}	25.17	***	74.83
PLA	29.23	***	70.77
K_{hp}	0.88	n.s.	99.12

944

945 **Table 3.** Scaling exponents of each leaf habit (deciduous and evergreen) separately for
 946 standardized major axis (SMA) regressions. All variables were log₁₀ transformed. The
 947 scaling relationship (isometry or allometry) was selected taking into account if the 95%
 948 confident interval of the slope includes the value 1 (isometry) or not (allometry). All
 949 correlations are significant ($P < 0.001$) but K_{hp} with LA. Leaf traits notation as in Table
 950 1. Differences in the slope and elevation between deciduous (DEC) and evergreen (EVE)
 951 species are shown with asterisks ($P < 0.001$ ***, $P < 0.01$ **, $P < 0.05$ *, NS = No
 952 significant).

y	x	Figure	Deciduous			Evergreen			DEC vs EVE	
			Slope	Scaling relationship	R ²	Slope	Scaling relationship	R ²	Slope	Elevation
A _{pet}	LA	Fig. 4a	0.73	Allometry	0.486	0.9	Isometry	0.752	*	***
A _c	LA	Fig. 4b	0.71	Allometry	0.816	0.79	Allometry	0.816	NS	***
A _x	LA	Fig. 5a	0.74	Allometry	0.874	0.76	Allometry	0.651	NS	***
d _{hx}	LA	Fig. 5b	0.33	Allometry	0.507	0.37	Allometry	0.563	NS	NS
XLA	LA	Fig. 5c	-0.4	Allometry	0.579	-0.59	Allometry	0.429	*	*
A _p	LA	Fig. 5d	0.75	Allometry	0.599	0.87	Allometry	0.69	NS	***
d _{hp}	LA	Fig. 5e	0.24	Allometry	0.2	0.24	Allometry	0.443	NS	*
PLA	LA	Fig. 5f	-0.63	Allometry	0.439	-0.56	Allometry	0.24	NS	NS
A _p	A _x	Fig. 51	1.01	Isometry	0.716	1.15	Allometry	0.811	NS	NS
K _{hx}	LA	Fig. 6a	1.57	Allometry	0.724	1.66	Allometry	0.56	NS	NS
K _{sx}	LA	Fig. 6b	1	Isometry	0.415	1.18	Isometry	0.281	NS	NS
K _{hp}	LA	Plot not shown	1.13	Isometry	0.276	1.61	Isometry	0.036	NS	NS

953

954 **Table 4.** Scaling exponents of physiological traits for standardized major axis (SMA)
 955 regressions. All variables were log₁₀ transformed. Leaf traits notation as in Table 1. Every
 956 correlation is significant ($P < 0.05$) and scale allometrically (slope significantly different
 957 of 1).

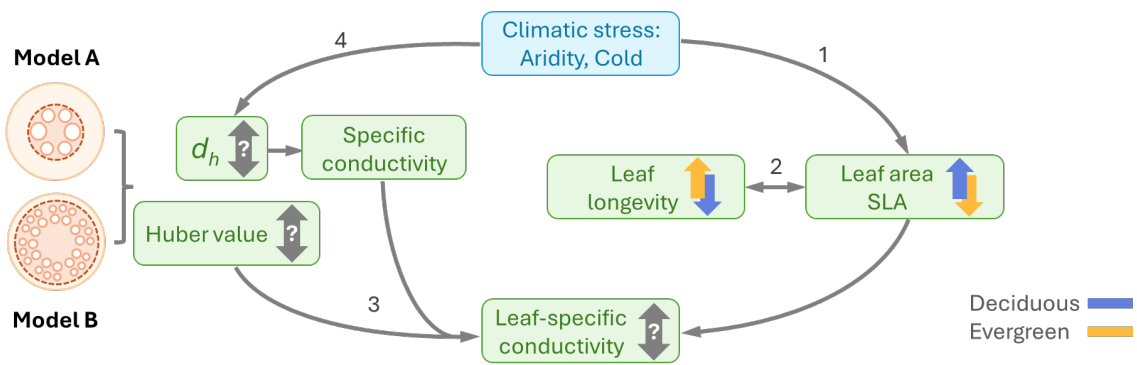
y	x	Figure	Slope	Scaling relationship	R ²
A _x	g_{s,leaf}	Fig. 8a	0.61	Allometry	0.512
d _{hx}	g_{s,leaf}	Fig. 8b	0.38	Allometry	0.586
K _{hx}	g_{s,leaf}	Fig. 8c	1.86	Allometry	0.684
A _x	A_{N,leaf}	Fig. 8d	0.63	Allometry	0.591
d _{hx}	A_{N,leaf}	Fig. 8e	0.39	Allometry	0.671
K _{hx}	A_{N,leaf}	Fig. 8f	1.91	Allometry	0.786
A _p	A_{N,leaf}	Fig. 9a	0.73	Allometry	0.561
d _{hp}	A_{N,leaf}	Fig. 9b	0.23	Allometry	0.509

958

959 **Table 5.** References of studies exploring the scaling relationship between xylem and
960 phloem conductive areas, specifying the species and organs studied as well as the slope
961 and the nature of the scaling found, either isometry or allometry.

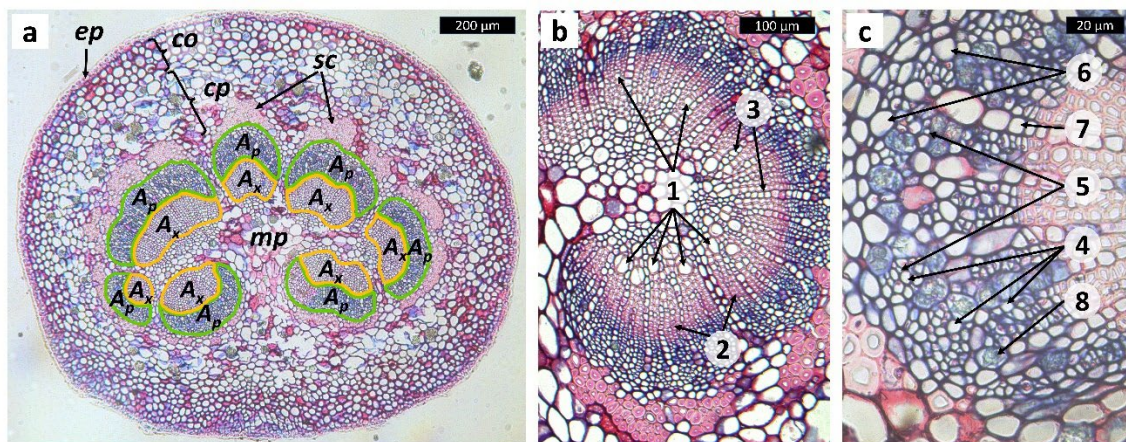
Reference	Species	Organ	Slope	Scaling relationship
Jyske and Hölttä 2015	<i>Picea abies</i>	Stem	0.93	Isometry
Carvalho et al. 2017a	<i>Populus × canescens</i>	Leaf, petiole	0.96	Isometry
Carvalho et al. 2017b	<i>Ginkgo biloba</i>	Leaf	0.91	Isometry
Kiorapostolou and Petit 2019	<i>Fraxinus ornus</i>	Stem	0.96	Isometry
962 Ray and Jones 2018	<i>Pelargonium</i> (11 spp.)	Petiole	0.87	Isometry

963



965

966 **Fig. 1.** Scheme of the traits that ultimately modulate the leaf-specific conductivity (LSC)
 967 of the petiole. Thick colored arrows show the tendency of each leaf habit (deciduous in
 968 blue and evergreen in orange) to have larger (upward arrow) or smaller (downward arrow)
 969 values for leaf longevity, leaf area and specific leaf area (SLA). Thick grey arrows
 970 represent the unknown relationships we aim to explore in this study. Two anatomical
 971 models are proposed: model A assumes that LSC can be improved increasing the
 972 hydraulic diameter (d_h), whereas model B assumes that for the same cross-section of
 973 petiole, a similar LSC could be reached by increasing the conductive area with a smaller
 974 d_h . References that support the proposed relationships are: 1) Sancho-Knapik et al.
 975 (2021); 2) Mediavilla et al. (2008) and Kikuzawa et al. (2013); 3) Mencuccini et al.
 976 (2019). 4) Blackman et al. (2023).

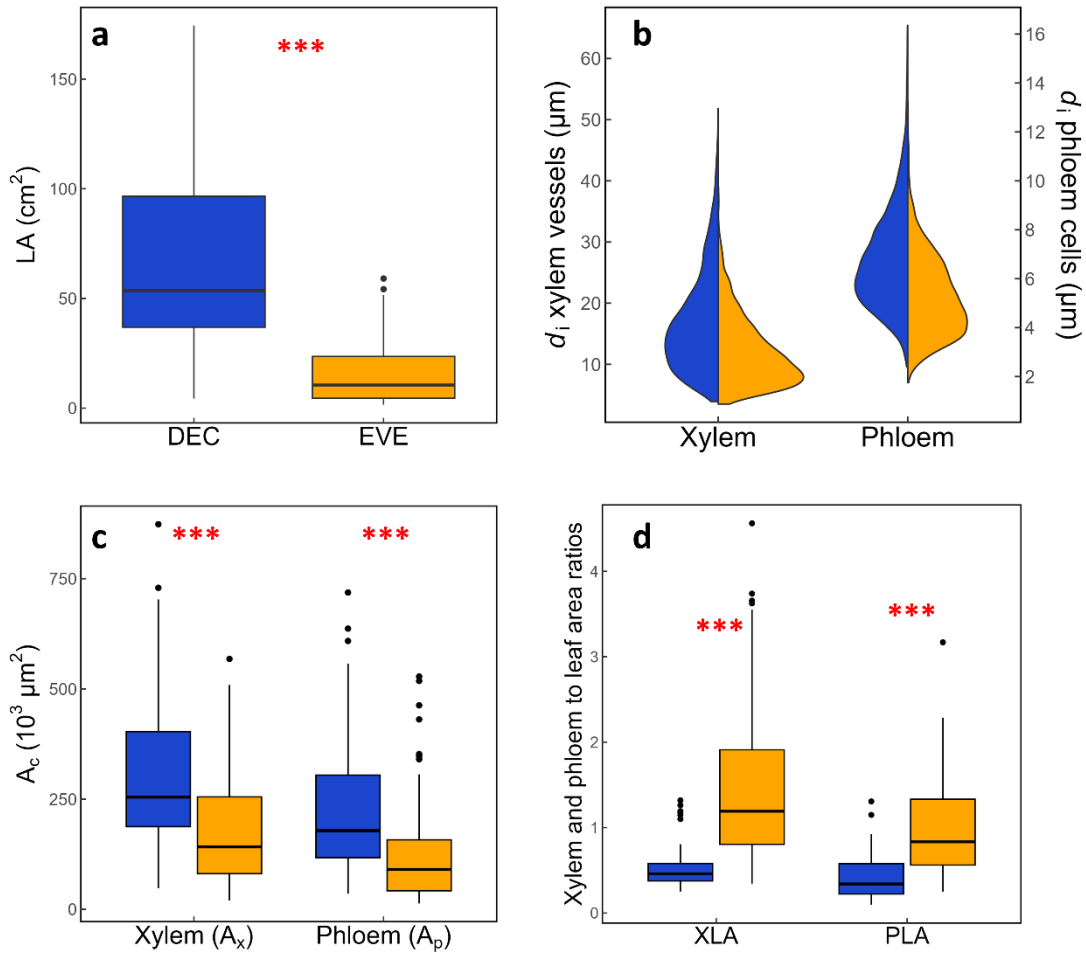


977

978 **Fig. 2.** Histological cross-section of *Quercus agrifolia* petiole. **(a) General scheme** of the
 979 whole petiole with the main tissues: epidermis (ep), collenchyma (co), cortical
 980 parenchyma (cp), sclerenchyma (sc), medullary parenchyma (mp) and the conductive
 981 tissues, measured in this study: xylem (A_x , highlighted in yellow) and phloem (A_p ,
 982 highlighted in green). **(b) Magnified view of xylem** with its main cellular types: xylem

983 vessels (1; measured in this study), tracheids (2) and parenchymatic medullary rays (3).
984 **(c) Detailed view of phloem** with its main cellular types: potential sieve tubes (4;
985 measured in this study), potential companion cells (5), phloem fibers (6), medullary rays
986 (7) and parenchyma (8).

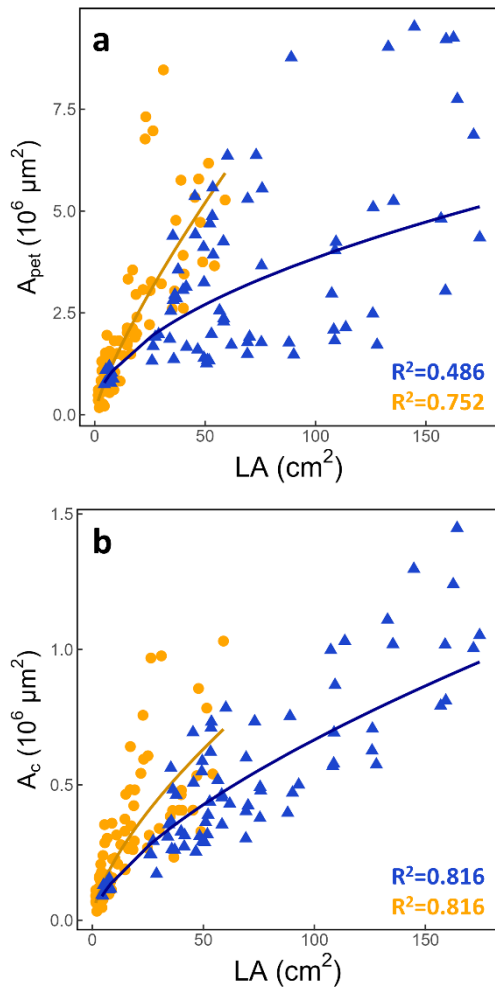
987



988

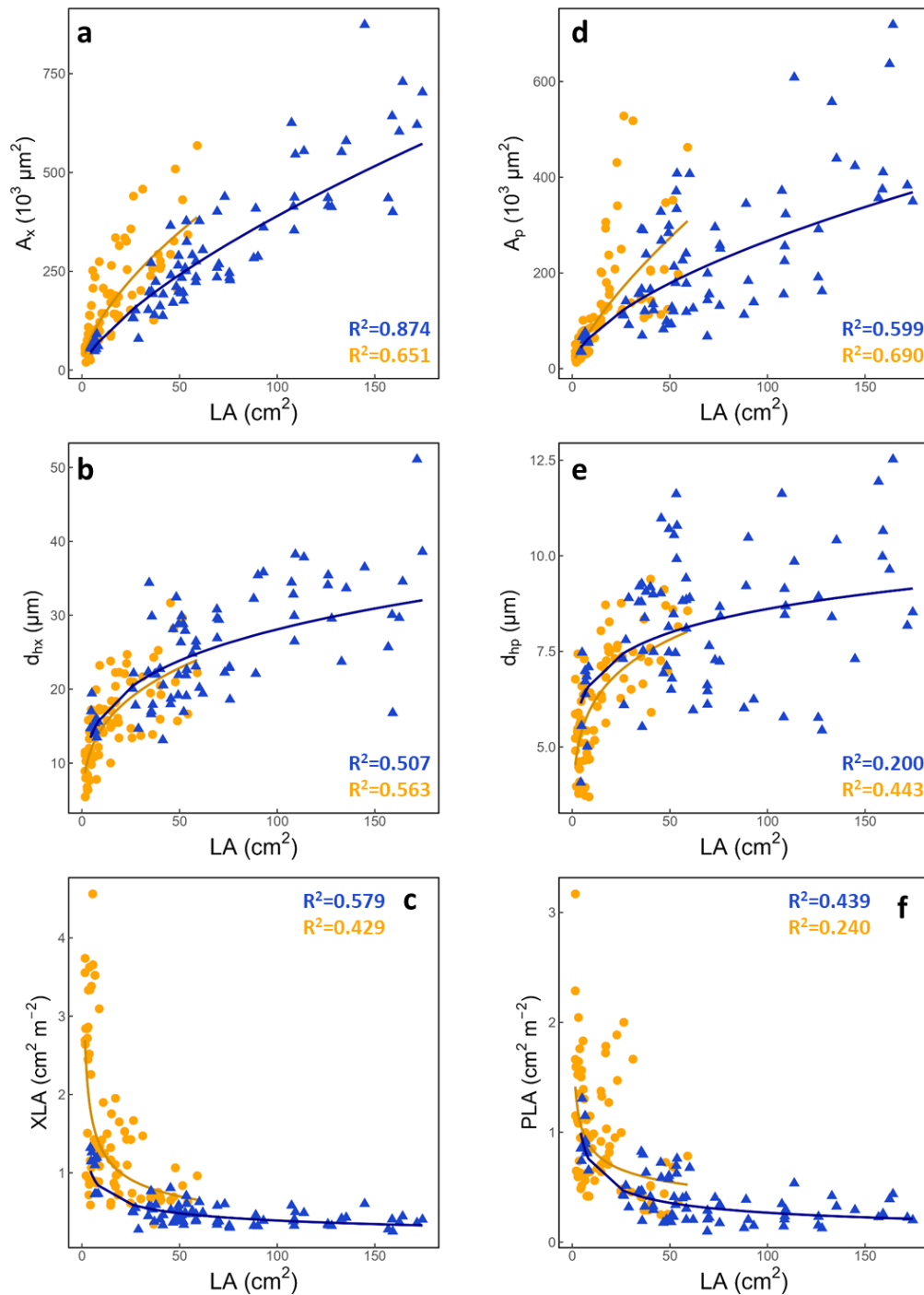
989 **Fig. 3.** Distribution of the main traits measured: a) Boxplot of the leaf area (LA), b) Violin
 990 plot of the diameters (d_i) of the conduits (vessels for xylem and sieve tubes for phloem),
 991 c) Boxplot total conductive area (A_c) in the petiole, and d) Xylem and phloem to leaf area
 992 ratios, i.e., conductive area divided by LA. Red asterisks show significant ($P < 0.001$)
 993 differences between leaf habits (blue, deciduous; orange, evergreen). Note the double Y
 994 scale in panel b).

995



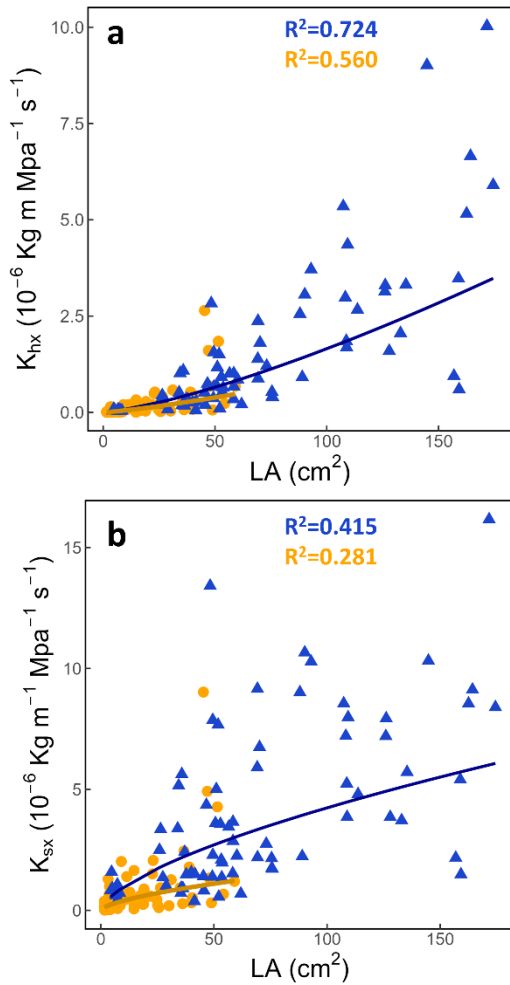
996

997 **Fig. 4.** Scaling relationships of a) leaf area (LA) with cross-sectional petiole area (A_{pet})
 998 and b) LA with conductive area (A_c , the sum of xylem and phloem areas) for deciduous
 999 (blue triangles) and evergreen (orange dots) species. Each point represents one individual
 1000 measure. Colored continuous lines represent the best fit for each leaf habit separately. All
 1001 regressions are highly significant ($P < 0.001$).



1002

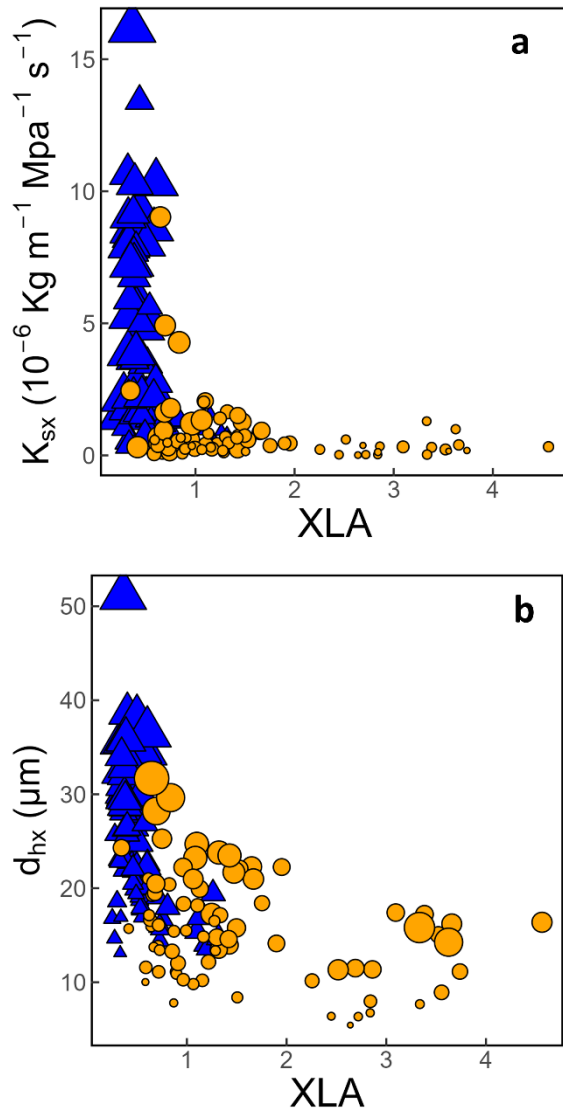
1003 **Fig. 5.** Correlations related to xylem (panels a-c) and phloem (panels d-f) anatomy for
 1004 deciduous (blue triangles) and evergreen (orange dots) species between leaf area (LA)
 1005 and: a) xylem cross-sectional area (A_x), b) xylem hydraulic diameter (d_{hx}), c) xylem cross-
 1006 sectional area divided by LA (XLA), d) phloem cross-sectional area (A_p), e) phloem
 1007 hydraulic diameter (d_{hp}) and f) phloem cross-sectional area divided by LA (PLA). Each
 1008 point represents one individual measure. Colored continuous lines represent the best fit
 1009 for each leaf habit separately. All regressions are highly significant ($P < 0.001$).



1010

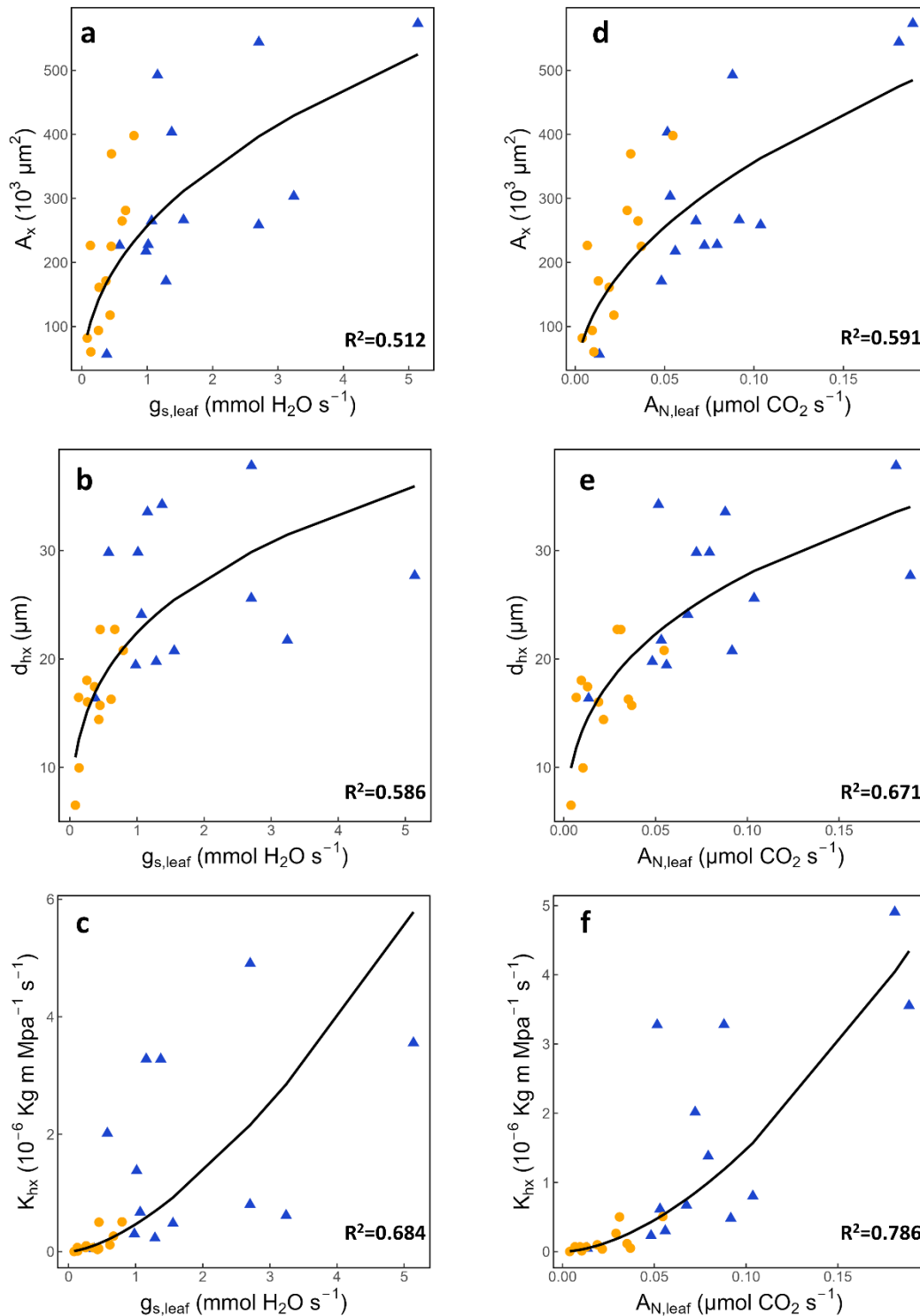
1011 **Fig. 6.** Correlations related to a) xylem hydraulic conductivity (K_{hx}) and b) specific
 1012 hydraulic conductivity (K_{sx}) for deciduous (blue triangles) and evergreen (orange dots)
 1013 species. Each point represents one individual measure. Colored continuous lines represent
 1014 the best fit for each leaf habit separately. All regressions are highly significant ($P < 0.001$).

1015



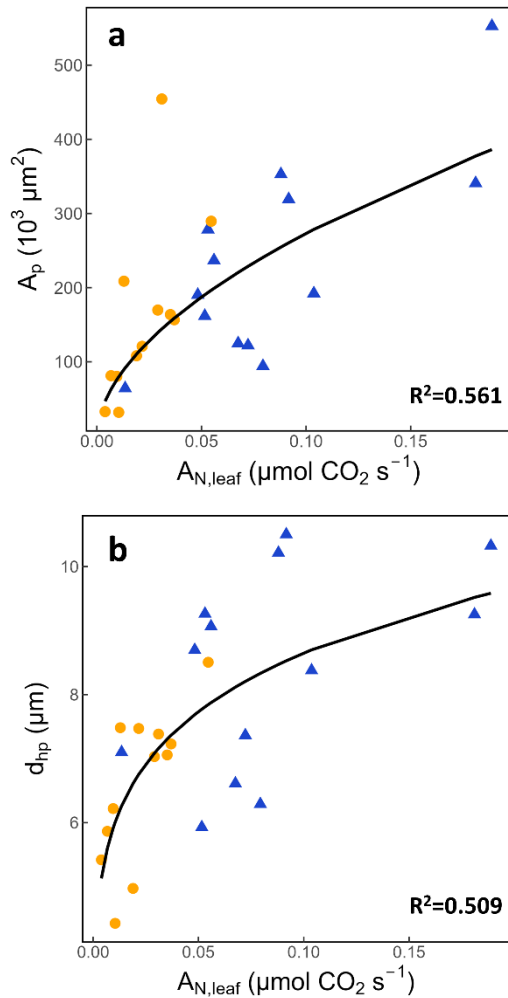
1016

1017 **Fig. 7.** Correlations between a) XLA and the xylem specific conductivity (K_{sx}) showing
 1018 the leaf area as the relative size of the symbols (larger symbols represent larger leaf areas);
 1019 and b) between the XLA and the xylem hydraulic diameter (d_{hx}) showing the leaf specific
 1020 conductivity (LSC) as the relative size of the symbols (larger symbols show higher LSC
 1021 values). Leaf habit is represented by deciduous in blue triangles and evergreen species in
 1022 orange dots. Each point represents one individual measure.



1023

1024 **Fig. 8.** Relationships between xylem traits (cross-sectional area (A_x), hydraulic diameter
 1025 (d_{hx}) and calculated hydraulic conductivity (K_{hx}), stomatal conductance ($g_{s,leaf}$) and
 1026 photosynthesis net rate ($A_{N,leaf}$). Blue triangles are deciduous and orange dots are
 1027 evergreen species. Each point represents the mean value of a species. The black
 1028 continuous line is the correlation considering species altogether. All regressions are highly
 1029 significant ($P < 0.001$).



1031

1032 **Fig. 9.** Main relationships between photosynthesis net rate ($A_{N,leaf}$) and phloem anatomical
 1033 traits (cross-sectional area (A_p) and hydraulic diameter (d_{hp})). Deciduous as blue triangles
 1034 and evergreen species as orange dots. Each point represents the mean value of a species.
 1035 The black continuous line is the correlation considering species altogether. Both
 1036 regressions are highly significant ($P < 0.001$).